Theses and Dissertations

2015

# New Quaternary geochronometric constraints on river incision in the Virginia Piedmont: Relative contributions of climate, base-level fall, knickpoint retreat, and active tectonics

Helen Fitzgerald Malenda
*Lehigh University*

New Quaternary geochronometric constraints on river incision in the Virginia Piedmont:
Relative contributions of climate, base-level fall, knickpoint retreat, and active tectonics

by

Helen Fitzgerald Malenda

A Thesis

Presented to the Graduate and Research Committee

of Lehigh University

in Candidacy for the Degree of

Master of Science

In

Earth and Environmental Sciences

Lehigh University

August 2015

Thesis is accepted and approved in partial fulfillment of the requirements for the Master of Sciences in Earth and Environmental Sciences

New Quaternary geochronometric constraints on river incision in the Virginia Piedmont: Relative contributions of climate, base-level fall, knickpoint retreat, and active tectonics

HELEN FITZGERALD MALENDA

_____

Date Approved

_____

Frank Pazzaglia

Advisor

_____

Stephen Peters

Committee Member

_____

Tammy Rittenour (Utah State University)

Committee Member

_____

David Anastasio

Department Chair

# ACKNOWLEDGEMENTS

TABLE OF CONTENTS

LIST OF TABLES

LIST OF FIGURES

ABSTRACT

River terraces are fluvial landforms that represent flood plains abandoned through river incision and, when accurately correlated and dated, can serve as paleogeodetic markers, indicating the elevation and location of past channels and the subsequent fluvial and tectonic processes shaping the landscape. Fluvial terraces are most useful when the incision processes that caused their abandonment and formation are better understood. This thesis studies river incision reconstructed from fluvial terraces of the South Anna River in the central Virginia Piedmont, USA. The South Anna River flows directly above an active fault, on which large, but infrequent seismic events have occurred, and the most recent event was the 23 August 2011 Mineral earthquake. Two conceptual incision models are tested to better understand the fluvial response to active tectonics in this region: 1) spatially-uniform vertical incision and 2) diachronous horizontal knickpoint retreat. Here, terraces and incision were evaluated in the context of a 1:24,000 scale surficial map of alluvial deposits, optically stimulated luminescence (OSL) and infrared luminescence (IRSL) geochronology, and knickpoint celerity modeling. The South Anna River and its tributaries traverse across the geologic, topographic and structural grain of central Virginia Piedmont, USA, a region known for Late Cenozoic base-level fall, high amplitude climate changes, and historic seismicity. Litho- and pedostratigraphically correlative deposits are found to form five groups of terraces (Qt1-Qt5) with similar, but not exact relative elevations above modern channel. Within these groups, the terraces have similar OSL/IRSL ages that do not systematically decrease in age upstream towards knickpoint in the modern channel. Similarly, the modeled rate of knickpoint retreat through the South Anna channel of ~7-14km/Ma is too slow to explain the time-transgressive OSL/IRSL dates for any terrace group. Terrace formation by knickpoint migration and horizontal

1

floodplain abandonment is rejected as a dominant process in terrace formation, in favor of more spatially-uniform vertical incision. In this landscape, the OSL/IRSL results suggest that flood plains are widened and then are abandoned and become terraces as the South Anna channel responds to climatically-driven unsteady changes in discharge and sediment yield. The complex age-elevation relationships of terraces proximal to epicenter of the 23 August 2011 Mineral earthquake argue for a terrace correlation that allows for rock uplift consistent with the co-seismic response of the 2011 Mineral earthquake.

INTRODUCTION

Over 50 years have passed since John T. Hack's seminal work (1957, 1960) investigating river drainages' longitudinal profiles of rivers in the Piedmont and Coastal Plain of Virginia and Maryland. From this work he was able to deduce empirical relationships between slope, area, and basin parameters that are key to modern fluvial research, including this study. The river systems of the region still proffer evidences key to answering a variety of relatively unexplored questions related to regional fluvial geomorphic evolution, incision history, and responses to intra-plate tectonics such as the observed seismicity in the Virginian Piedmont.

River incision is an inherently dynamic and unsteady process (Shepard and Schumm, 1974; Womack and Schumm, 1977; Frankel et al., 2007) that modifies fluvial systems and in doing so, produces terrace profiles with morphologies that can vary from the current river profile. Two end-member incision models: 1) spatially-uniform vertical incision and flood plain abandonment and 2) diachronous horizontal knickpoint retreat, are tested for their relative roles the formation of strath terraces along the South Anna River, Virginia, USA. Both forms of terrace genesis are plausible in the central Virginia Piedmont as the east coast of the United States (ECUS) has undergone Late Cenozoic glacial-interglacial cycles (Boettcher and Moilliken, 1994; Peizhen et al., 2001; Molnar, 2004; Reusser et al., 2004; Ward et al., 2005; Hancock and Kirwan, 2007) as well as Neogene to recent uplift, evidenced by long-wavelength perturbation of land surface elevations and geomorphic markers (Vogt, 1991; Pazzaglia and Gardner, 1994; Pazzaglia and Brandon, 1996; King, 2007; Rowley et al., 2013). Lithospheric uplift and possible far-field stresses has been

proposed as a source of observed intraplate seismicity in the Mid-Atlantic region, the genesis of which is still debated (Wolin et al., 2012).

The South Anna River flows southeast from the Blue Ridge through the central Virginia Piedmont and runs through the Central Virginia Seismic Zone (CVSZ) and directly over the fault plane of the 2011 Mineral earthquake (Berti et al., 2015). The fault strikes N 36 °E and dips 49.5° east-southeast (McNamara et al., 2014), and the hanging wall rises downstream of the footwall. The river traverse orthogonal to the reverse fault plane offers a rare opportunity to study fluvial responses to active tectonics in the intraplate setting of the ECUS. To better use reconstructed terrace profiles along the South Anna River as paleogeodetic markers in tectonic studies, the dominant background fluvial responses to the unsteady Late Cenozoic climate and base-level fluctuations and the dominant mechanism in terrace formation are examined using surficial litho- and chronostratigraphic constraints.

The observation of reoccurring seismicity on the ECUS remains forefront in research (see GSA Special Publication 509; Burton et al., *eds*, 2015), because besides the observed earthquakes, little evidence is offered about their genesis, or long term reoccurrence patterns (Wolin et al., 2012). Unlike active boundaries, there is no general model for intraplate seismicity nor for the focusing of plate interior deformation, although general hypotheses involving legacy structure reactivation (Wheeler and Bollinger, 1984; Hatcher et al., 1987; Seeber and Armbruster, 1989; Thomas, 2006) or fault-healing processes (Ebel, 2009; Stein and Liu, 2009) have been proposed. Additionally, although moderate to large seismic events appear to cluster regionally, there are no overt surface expressions to indicate co-seismic strain accumulation along active faults (Wolin et al., 2012). This study

potentially offers clarification of the dominant fluvial mechanisms involved in floodplain abandonment and terrace formation in the central Virginia Piedmont. This greatly increases the impact of using terraces in this region as paleogeodetic markers and gives an estimation of fluvial response and deposit modification to repeated tectonic activity in the CVSZ. The lithostratigraphy can also be applied to future paleogeodetic studies of terrace deposits in other seismically active areas in the CVSZ.

The two-dimensional and unsteady nature of incision may result in suites of terraces that are not equal in preservation or spacing. Terrace deposits must be accurately characterized, mapped, and dated before longitudinal analyses of river channels and their respective terrace deposits can be used to quantify the horizontal and vertical components of river incision. The goal of this research is to better resolve terrace formation mechanisms and inform paleogeodetic studies using terraces in the Virginia Piedmont. In order to do so, 1) a field campaign was launched including detailed descriptions and stratigraphic analyses of fluvial deposits along the South Anna River, in Louisa County, Virginia, USA). Field data is used to quantify the gradients and elevation (both absolute and relative to the current channel) of each terrace and to construct the development of a portable lithostratigraphy; 2) knickpoint celerity is modeled using a stream power erosion law to constrain rates of horizontal migration of transient incision designed to predict the diachroneity of terraces that would emerge via the knickpoint retreat process; and 3) OSL and IRSL geochronology is employed to date deposits and compare ages to the spatial transience predicted by the celerity modeling. Only after the fluvial mechanisms in terrace formation are better understood, can unresolved observations of terrace age-elevation relationships and

locations be utilized to interpret the role the active tectonics play in terrace preservation and post-deposition modification.

FLUVIAL INCISION MODELS

In fluvial systems exogenic climate forcing can cause changes in discharge, sediment load, and sediment size. The interplay between these parameters results in variability in effective stream power and channel insulation, which dictate either lateral planation of straths or vertical incision and strath abandonment (Gilbert, 1877; Bull, 1991; Mackin, 1937; Wegmann and Pazzaglia, 2002; Hancock and Anderson, 2002; Fuller et al., 2009). Terrace suites, particularly those paired in a river valley, are believed to be the sum of protracted periods of lateral planation and relatively short periods of rapid vertical incision and terrace formation (Wegmann and Pazzaglia, 2002; Hancock and Anderson, 2002; Fuller et al., 2009). Lateral planation occurs during periods of low effective discharge and subsequent channel insulation, and rapid vertical incision happens during periods of increased stream power and/or channel bedrock access (Hancock and Anderson, 2002). High-amplitude Late Cenozoic glacial-interglacial cycles may have modulated both the amount of water available to fluvial systems through glacial arrest and melt, as well as the sediment supply through enhanced erosion or colluviation (Bull, 1991; Wegmann and Pazzaglia, 2002; Hancock and Anderson, 2002; Ward et al., 2005; Hancock and Kirwan). Over geologic time, climate forcing could result in regional trends in temporally-unsteady vertical incision rates and terrace preservation (Shackleton et al., 1984; Molnar and England, 1990; Zhang et al., 2001).

Although the ECUS is thought of as an "archetypal" passive margin (Fail, 1998) the region has experienced uplift and subsequent base-level fluctuations since the Late Cenozoic

(Davis 1889; Hack, 1982; Pazzaglia and Gardner, 1994) which may be the combined effect of load-related lithospheric flexure (Pazzaglia and Gardner, 1994; Pazzaglia and Brandon, 1996) and dynamically-supported topography (Moucha et al., 2008; Rowley et al., 2013). Recent numerical studies of passive mantle flow and dynamic topography (Moucha et al., 2008; Spasojević et al., 2008; Rowley et al., 2013) are significant, because they imply active far-field lithospheric stresses acting on the CEUS. This additional component of lithospheric deformation has been proposed as a source of observed intraplate seismicity in the Mid-Atlantic region, the genesis of which is still debated (Wolin et al., 2012).

Base-level falls, the possible outcome of rock uplift and/or sea level variation, result in acute readjustment of a river through rapid local incision and the formation of a knickpoint (Gardner, 1983; See Kirby and Whipple, 2012). The knickpoint propagates diachronously upstream at a rate dictated by rock type, local slope, and drainage area (Hack, 1975; Seidl and Dietrich 1992; Zaprowski et al., 2001, Crosby and Whipple, 2006). Consequently, the wave of incision and terrace abandonment creates an adjusted reach and time-transgressive strath terraces downstream of the knickpoint and an un-incised reach upstream (Figure 1). Regionally, there are many predominant knickpoints observed along the ECUS (Walter and Merritts, 2008; Pazzaglia and Gardner, 1994; Miller et al., 2013; Berti et al., 2015), which could be the manifestation of transient fluvial response to base-level falls via knickpoint formation and migration. Alternatively, these knickpoints could be stationary, reflecting local geological or structural disparities in erodibility (Hickock, 1933). Consequently, the retreat of rapidly incising knickpoints is a possible mechanism for terrace abandonment and preservation of horizontally time-transgressive terraces (Crosby and Whipple, 2006; Frankel et al., 2007), which can be supported or refuted by the

synthesis of geochronological data and time constraints provided by numerical knickpoint celerity modeling (Rosenbloom and Anderson, 1994; Whipple and Tucker, 1999; Berlin and Anderson, 2007; Crosby and Whipple, 2006).

Well-studied and biostratigraphically-constrained Coastal Plain stratigraphy provides litho- and chronostratigraphy necessary for the separation of cumulative coastal lithospheric uplift (both flexural and dynamically-supported) from eustatic fluctuations (Pazzaglia, 1993; Dowset and Cronin, 1990; Wehmiller et al., 1988) and an explanation of observed sea-level curve variability along the ECUS (Pazzaglia and Gardner, 1994; Pazzaglia and Brandon, 1996; Moucha et al., 2008; Rowley et al, 2013). Therefore, the coastal marine deposits are important paleogeodetic markers, and additionally, can be correlated with east coast fluvial deposits or knickpoints, such as those observed along the South Anna River to inform interpretations about inboard fluvial stratigraphy and incision histories (Pazzaglia, 1993; Dowset and Cronin, 1990; Wehmiller et al., 1988).

SETTING

*Geology, Topography, Climate*

The study area is located in the central Virginia Piedmont, approximately 60 kilometers northwest of Richmond, Virginia, and 150 km southwest of Washington D.C. (Figure 2). The geologic and topographic fabric of central Virginia strikes northeast-southwest, and is sub-parallel to the coast, reflecting the region's tectonic history. Late Proterozoic to early Paleozoic metamorphic and metavolcanic terranes underlie the majority of the study area, and represent compression and suturing of the protracted assembly of Pangaea (Pavlides, 1989, 1990, 1995; Horton et al., 1989; Pavlides et al., 1994; Mixon et al., 2000, 2005; Spears et al., 2002; Spears and Gilmer, 2012; Hibbard et al., 2013; and Hughes et al., 2013).

The surficial mapping component of this work is exclusively in Louisa County, VA, which is underlain by rock-types related to the Taconic Orogeny (Horton et al., 1989; Hibbard et al., 2007; Thomas, 2006; Hatcher, 2010; Sinha et al., 2012). They are (from northeast to southwest): the Proterozoic-Pennsylvania Green Springs Pluton of diorite and hornblendite emplaced in Proterozoic-Ordovician meta-greywackes and mélange; the Ordovician-Silurian Ellisville biotite and granodiorite; and the Chopawamsic terrane composed of the Cambrian Chopawamsic mafic-felsic, mica-rich metavolcanics and the Ordovician Quantico garnet-mica schist. Downstream of the mapping area are tributaries of the South Anna River which were included in desktop knickpoint celerity modeling. Here, the Alleghenian-related Falmouth intrusive suite of granites, granodiorites, and tonalities of the Goochland terrane (Horton et al., 1989; Hibbard et al., 2007; Thomas, 2006; Hatcher, 2010; Sinha et al., 2012) divide the lithologies of the aforementioned Chopawamsic terrane from Proterozoic-Cambrian gneisses and cataclastic rocks to the southwest (Figure 2).

9

Although these metamorphic terranes are heterolithic, they have similar erodibilities, resulting in an erosionally-uniform landscape in the study area. Multiple lithologies in the study area are bounded by high-angle faults (Figure 2; Harris et al., 1982, 1985; Keller et al., 1985; Pratt et al., 1988; Lampshire et al, 1994; Pratt et al., 2015) for which the timing of (re)activation remains a current area of study (Hughes et al., 2013).

During the Pleistocene the mid-Atlantic region experienced multiple glacial and interglacial cycles, which increased in amplitude and frequency in the Late Pleistocene (Pagani et al., 2002). The furthest glacial advance terminated in northern Pennsylvania, approximately 350 km north of the study area, and the study area was impacted by periglacial cold-climate geomorphic modifiers (Clark and Ciolkosz, 1988; Whittaker and Ryter, 1992), such as enhanced colluviation (Eargle 1977), mass wasting (Mills 1988), and solifluction (Delcourt and Delcourt, 1985).

*South Anna River Basin*

This study focuses on the South Anna River and its tributaries (Figure 3), the headwaters of which originate east of the Blue Ridge. The main channel joins the North Anna, Little, Newfound, and Paumunky Rivers northeast of Richmond, Virginia, marking the beginning of the York River, which continues on to the Atlantic Ocean. The main channel of the South Anna River flows southeast, perpendicular to the geologic and topographic strike. Because of its aspect relative to the geological and structural grain, the South Anna River encounters many lithological contacts and structural features, such as faults. The South Anna River traverses the 2011 Mineral earthquake epicenter, and flows orthogonal to the relevant southeast-dipping reverse fault, a relationship that inspired the detailed geomorphic study and surficial mapping initiative included in this study. There are

10

multiple knickpoints (Figure 3) and co-located anthropogenic mill dams, which capitalized on the increased potential energy across the head drop along the main channel and tributaries of the South Anna River (Walter and Merritts, 2008).

Through river profile reconstruction (Goldrick and Bishop, 1995; Schoenbohm et al., 2004; Clark et al., 2005; Berlin and Anderson, 2007; Harkins et al., 2007; Kirby and Whipple, 2012; Miller et al., 2013) major knickpoints along the South Anna River can be correlated to the well-studied and biostratigraphically-dated marine deposits of the Coastal Plain (Figure 3; Dowsett and Wiggs, 1992; Pazzaglia, 1993). The Middle Miocene (11.5-13 Ma; Andrews, 1976; Carter et al., 2007) Choptank Formation, and the Early Pliocene (3.5-5 Ma; Dowsett and Wiggs, 1992) Yorktown Formation are respectively correlative to the 150m and 52m (elevation) knickpoints along the South Anna River (Figure 3). The ages of these formations represent upper age limits of marine deposit abandonment via base-level fall and the initiation of rapid vertical incision and knickpoint formation. Abandonment represents the initiation of channel adjustment along the South Anna River via the respective knickpoint, and the age of the formation therefore represents the time it took the knickpoint to migrate from the coast to its current location (either at 52 or 150m elevation).

METHODS

*Field Studies and Mapping*

Surficial mapping of alluvial deposits in the Virginia Piedmont presents a variety of challenges related to the near ubiquitous vegetative cover, low relief, and general lack of natural exposure. In addition, post-depositional modification of alluvial deposits by natural colluvial processes, significant anthropogenic modifications to the landscape by centuries of farming, logging, and construction, and controlled access to private property contributed to the mapping challenges.  Use of maps, airphotos, and other lab-based datasets helped meet these challenges and reduce the degree of uncertainty in deposit location and extent.

Key to the surficial mapping methods was establishing a protocol for communicating uncertainty in deposit origin, location, and elevation. The criteria used in this protocol are presence or absence of a terrace morphology, Natural Resource Conservation Service (NRCS) mapped soils (Masada, Turbeville, Forks, and Altavista) associated with an alluvial parent material, field confirmation of gravel and associated alluvial material, concordant elevations of adjacent or paired terraces, and the integration of previous observations assembled on Virginia Department of Mine, Minerals, and Energy (VA DMME) and United States Geological Survey (USGS) maps. Three categories of map unit confidence emerged from this exercise: confirmed alluvial terrace deposit with a well constrained basal unconformity (strath) separating alluvium from underlying bedrock or saprolite (C1), likely alluvial terrace deposit modified by colluvial or anthropogenic processes and an obscured strath (C2), possible alluvial deposit heavily modified by colluvial or anthropogenic processes, lacking an intact strath (C3).  These different levels of confidence are communicated using coordinated deposit outlines on the map (Appendix

12

A), and only the units with the highest degree of confidence (C1) were used in subsequent terrace correlations presented in this study.

*Map-based observations*

Mapping was conducted in the Ferncliff, Pendleton, and the top portion of the South Anna quadrangles, Virginia at the 1:24,000 scale on a base of standard paper 7.5 minute USGS quadrangles with 10-foot (3 m) contours, accompanied by GPS-guided locations provided by the GaiaGPS app on an iPad. Alluvial deposits were first identified by their morphology, a broad flat surface tread commonly flanked by terrace risers. This morphology is underlain by alluvial deposits typically < 2 m thick.

NRCS soil data available on the web (http://websoilsurvey.sc.egov.usda.gov/App/Home Page.html) were also utilized to provide an independent assessment of the distribution of alluvial parent materials to the Virginia Piedmont soils. A distinction was made in the field between soils that were intact with an underlying alluvial parent, from those that were primarily colluvial, mixing alluvial, residual, and bedrock parent materials. Given the generally poor exposures of alluvial deposit straths, a strategy was adopted to pick the strath elevation based on the upslope maximum elevation of gravel emerging from a hillslope underlain by alluvium. Vegetation changes and springs from perched aquifers sometimes aided in picking the strath. Strath elevation is picked to the nearest contour line (10-foot, 3.05-m contour interval) with uncertainties reported as ± one contour line.

Where possible, advantageous natural exposures, such as steep slopes, road cuts, and excavation, were utilized to observe deposit characteristics, stratigraphy, and deposit elevation. However, the majority of the textural and sedimentological descriptions are

summarized from frequent augering using a 4-inch diameter hand auger that penetrated to a depth of approximately 1 m.

*Gravel Textural and Compositional Analyses*

Textural and compositional data for deposits were collected to provide a quantitative and comparable basis for developing a lithostratigraphy and terrace correlation. Previous studies which investigated particle and particle-size distributions in fluvial settings (Bunte et al., 2001), as well as alternative photogrammetric approaches by the USGS (Warrick et al., 2009), set the framework for the compositional and textural analysis and the development of an efficient, software-based photogrammetric technique (Raup, 2014). The analyses were predicated on the assumptions that (1) the fluvial processes that transport gravels also round gravels, (2) gravel sourcing may have changed through time creating contrasting compositional makeups of the deposits (3) weathering of the deposits may create diagnostic signatures such as staining and/or weathering rinds.

Development of the photogrammetric technique was the focus of an unpublished senior thesis project (Appendix B; Raup, 2014) aimed at creating an efficient and reproducible digital approach to clast analysis. The deposits' textures were described by commonly used sedimentological qualities: roundness, circularity (similar to shape factor), and size. Roundness and circularity, given in percentages, were analyzed non-parametrically by grouping the results of 16 samples (Appendix C) into low (<70%), medium (70-75%) and high (>75%) categories. The clasts' areas, given in cm$^2$ were compared, and those samples which had areas within 2 cm$^2$ of one another were highlighted for further comparison. Once the clasts were analyzed for textural characteristics, they were broken open, sorted by lithology, and described. Characteristics that were noted included the friability of the

quartzites, patinas, red and/or ochre staining, and the presence and thickness of iron-rich weathering rinds.

Terraces were characterized using the aforementioned suite of field observations and laboratory data, which included the deposits' morphology, texture, composition, and pedogenic development.

*Luminescence Dating*

Depositional age estimates for terraces of various elevation along the South Anna River were determined using OSL (Huntly et al., 1985) and IRSL (Hütt, 1988) dating. Sampling site considerations were exposure, confidence of stratigraphic position, clear distinction in relative stratigraphic age, and broad distribution along the South Anna (Figure 4). Where natural vertical exposures were absent, 1-1.5 m pits were excavated to reach the target horizons. Stainless steel tubes were driven into sand lenses in the gravel deposits stratigraphically overlaying saprolitic bedrock straths. Sediment within 20 cm of each sample tube was collected for dose rate determination and measurement of water content.

The samples were processed and analyzed at the Utah State University Luminescence Laboratory, under darkroom conditions and in accordance with standard sample preparation procedures (Aitken, 1998; Rittenour et al., 2005). Samples were wet sieved to two target sizes: 75-150μm and 150-250 μm, were washed in HCl and floated in 2.7 g/cm$^3$ sodium polytungstate to extract quartz fractions for OSL dating and 2.58 g/cm$^3$ sodium polytungstate to extract potassium feldspar fractions for IRSL dating. The quartz fractions for OSL analysis were additionally treated with 47% HF to remove feldspars and etch the quartz grains. Values for dose rate were calculated from cosmic-ray contributions (Prescott

and Hutton, 1994), sediment water content (Aitken, 1998), and radioelemental concentration of the surrounding sediment using ICP-MS and ICP-atomic emission spectroscopy (ICP-AES) techniques and conversion factors (Guerin et al., 2011).

Samples were analyzed using the single-aliquot regenerative-dose (SAR) method (Murray and Whintle, 2000) for quartz and the post-infrared-IRSL (pIR-IRSL) technique (225°C stimulation) for feldspar (Buyleart et al., 2009). The equivalent dose (De) for each sample was calculated using the central age model (CAM; Galbraith et al., 1999). Due to saturation of the quartz signals, pIR-IRSL results are favored over quartz OSL in the oldest terrace samples.

*Knickpoint Celerity Modeling*

Knickpoint celerity modeling can aid in terrace correlation by informing the rate of horizontal incision. When coupled with age measurements of terrace deposits along the channel, knickpoint celerity modeling also allows a first order timescale estimate of transient incision and initial base-level fall (Kirby et al., 2010; Kirby and Whipple, 2012; Miller et al., 2013).

Knickpoint celerity modeling is part of a well-established body of river profile analyses founded in a family of stream-power and incision equations that depict relationships between discharge, drainage basin area, and bankfull-width (Snyder et al., 2000, Whipple, 2001, 2004; Kirby and Whipple, 2012). These equations are based on a semi-empirical relations between channel hydraulic geometry, water mass and momentum, and shear stress. The cumulative, stream power law:

$$E = K A^m S^n \qquad\qquad (1)$$

describes erosion ($E$) as a function of upstream drainage area ($A$) and channel slope ($S$). ($K$) is a proportionality constant related to rock properties that dictate the amount of rock that may be erode per unit shear stress or stream power, ($m$) and ($n$) are power-law constants on area and slope (Hack, 1973; Flint, 1974).

This study identifies genetically-related knickpoints, which are initiated from a common base-level fall, and time-transgressively migrate upstream at a rate dictated by the physical parameters of the basin, namely drainage area, which controls discharge (n=1; Niemann et al., 2001; Harkins et al., 2007; Berlin and Anderson, 2007; Crosby and Whipple, 2006):

$$dz/dt = KA^m \, dz/dx \qquad\qquad (2)$$

and

$$dx/dt = K \, A^m \qquad\qquad (3),$$

where ($dz/dt$) is the change in elevation over time; ($dz/dx$) is the change in slope; and ($dx/dt$) is the change in horizontal position over time. Knickpoints migrate horizontally at differential rates dependent on drainage area (eq 3), but because of the inverse scaling of drainage area and slope on incision, undeformed knickpoints climb at a constant vertical rate (eq 2; Figure 5). Therefore, potentially genetically-related knickpoints along various tributaries of the South Anna River were identified by their shared elevations, regardless of the size of the drainage (Wobus, et al., 2006; Kirby and Whipple, 2012).

Three candidate knickpoints found on multiple tributaries and the South Anna River were included in modeling: an approximately 52m elevation knickpoint on the main trunks of Beech Creek, Taylor Creek, and Cedar Creek; a 75 *m* knickpoint located on tributaries of Taylor Creek and Owens Creek, and an 85m knickpoint along tributaries of Owens Creek

(Figure 6). From a common base-level at the confluence of the tributaries and the South Anna River, the stream-power family of equations (eq 2 and 3) were applied to long profile data extracted from 10m DEMs in ArcGis and smoothed using a median (0.025) filter. A FORTRAN model developed in house (Appendix F; Pazzaglia et al., 2014) uses the distance, elevation, and area data from long profiles of three tributaries as inputs to predict the leading edge of the migration of a given knickpoint moving as a wave of incision up the tributaries (Rosenbloom and Anderson, 1994; Whipple and Tucker, 1999). The model requires the horizontal locations of the knickpoint ($x$; from the common base-level) along three tributaries, as well as the incremental channel elevation ($dz/dx$) and contributing drainage area ($A$) along each channel profile. Given current channel gradients and contributing upstream drainage areas of the three tributaries, the knickpoint's horizontal locations can be solved as a function of time (Niemann et al., 2001) by iterating through pairs of $K$ and $m$ values to find a combination that minimizes the root mean square error (the misfit) between predicted and observed distances of the knickpoint along the three drainages (Crosby and Whipple, 2006; Berlin and Anderson, 2007; Whittaker and Boulton, 2012; Schmidt et al., *in progress*). If the observed knickpoints are not related to a common base level fall or are locally reflective of rock type changes, the model may not converge, or there will be a large misfit between the predicted and observed locations in this test. Misfits do not have a unique explanation, and could be due to the starting resolution of the DEM, subsequent data smoothing, or unknown channel modification (Miller et al., 2013). If found to be genetically-unrelated, the horizontal locations of the knickpoint can be compared to the local geology using ArcGIS, to rule out bedrock contacts causing the knickpoints' arrest.

If the model-generated *K* and *m* pairs accurately predict locations of the knickpoint along the tributaries, (thus supporting a genetic relationship) the values can then be applied to the main channel, or an independent channel, to predict the horizontal location of a given knickpoint for a given time. An accurate prediction of the modeled knickpoint location on long profiles independent of the three modeled profiles corroborates the genetic relationship between the four knickpoints (the three used in the modeling, and the one used in the test) and assesses the validity of the *K* and *m* values' wider application throughout the drainage network. The Newfound River was used as the independent stream channel on which ability of the *K* and *m* combinations was tested to accurately predict the horizontal location of the knickpoint, which is represented by the model misfit.

The knickpoint celerity analysis was predicated on age constraints from an initial correlation drawn between the 52m knickpoint on the South Anna's main channel, and the 3.5-5 Ma Yorktown Formation of marine deposits on the Coastal Plain. The association between the knickpoint and coastal deposit was formed by reconstructing the relict channel profile using values for concavity and steepness representative of the unadjusted channel reach above the highest observable knickpoint (Figure 3; Miller et al., 2013; Berti et al., 2015). The age of the Yorktown Formation represents upper age limits of the coastal deposit abandonment via vertical incision in response to base-level fall. This abandonment represents the initiation of channel adjustment along the South Anna River via retreat of the 52m knickpoint, and the age of the Yorktown Formation therefore represents the time it took for the 52m knickpoint to migrate from the coast to its current location.

The key reason for modeling the 52m knickpoint was to aid in constraining a time input needed for two additional models of the 75m and 85m knickpoints on the Owens Creek

tributaries. Additional models were run, because although the 52m knickpoint was tested on the independent Newfound River, the stream data of the three tributaries shared a reach of South Anna River. In addition to the Newfound River, the $K$ and $m$ outputs of each celerity model, (the 52m on Beech, Cedar, and Taylor Creeks, 75m on the Owens Creek tributaries, and 85m knickpoint on the Owens Creek tributaries) were also used to predict the time needed for a knickpoint at current elevation of 150m along the South Anna to travel from base-level at the river mouth where the correlative marine terraces of the Choptank Formation biostratigraphically dated to be 11.5-13 Ma (Andrews, 1976; Carter et al., 2007). Similar to the Yorktown Formation, the age of the Choptank Formation represents the maximum age of the initial base-level fall, and the time it took the 150m knickpoint to migrate through the South Anna River channel. The biostratigraphic age range served as the tolerance limits for the time predicted by a given pair of $K$ and $m$ values' of base-level fall and knickpoint migration duration responsible for the 150m knickpoint (Figure 3; Berti et al., 2015); only the $K$ and $m$ values that satisfied these constraints were retained.

RESULTS

*Field Observations*

Alluvial deposits have long been recognized and mapped in the central Virginia Piedmont (NRCS; Howard et al., 1993; Weems, 1988; Spears et al., 2013; Berti et al., 2015), but there is little consensus on the appropriate geomorphic model for their identification, origin, age, and role in long term landscape evolution. The detailed mapping campaign included in this project offered an opportunity to develop portable criteria for distinguishing alluvial deposits that have been mobilized and deposited in the landscape by rivers and streams, from common accumulations of lag quartz gravel, and colluvium.

In addition to the mapped terraces, The main non- fluvial geologic units identified during field mapping were unweathered, foliated bedrock (Hughes, 2011; Hughes et al., 2015; Spears et al., 2013; Burton et al., 2015); saprolite; residual soil including quartz lag gravel; scattered, isolated extrabasinal clasts of rounded Antietam Quartzite; and a mixed-source colluvium derived from saprolite, bedrock, residual soil, and terrace alluvium.

Bedrock is poorly exposed in the Virginia Piedmont, outcropping only on very steep slopes, the outsides of steep meander bends of the South Anna River and its major tributaries, and less commonly in the escarpments between adjacent terrace levels (Figure 7). Veins of polycrystalline quartz, a common component of the local bedrock, protrude from both steep and gentle slopes and are a local source of angular to subrounded quartz gravel found in residual, colluvial, and alluvial deposits. The vein quartz in this part of the Virginia Piedmont is notable for being coarsely-crystalline and translucent, rather than the more common massive, opaque, crytocrystalline "bull quartz" variety.

The regional bedrock has been chemically weathered into saprolite, the depth of which is highly non-uniform and likely reflects water migration pathways that are locally controlled by fracture density, shear zones, and permeability contrasts. The saprolite has a structured texture close to the lower bedrock interface and progressively transforms into a more massive texture near the upper interface with a residual soil. Modeled assuming a steady-state relationship between the long term conversion of rock to saprolite, saprolite to residual soil, and removal of residual soil by erosion, the mean residence time of saprolite and residual soil in the Virginia Piedmont landscape is reported to be ~800 ka (Pavich et al., 1985). Accordingly, the conversion of rock to saprolite, saprolite to soil, and removal of soil by erosion is thought to occur at a rate of ~4.5 m/Ma.

Alluvial deposits are introduced to the Piedmont landscape by rivers and streams that recruit weathered materials from saprolite and residual soils; subsequently, materials can also be recruited from older alluvial deposits. The typical stratigraphy of the floodplain is < 2 *m* of clast supported, stratified sandy gravel channel facies overlain by 1-2 *m* of stratified, sand-silt and clay overbank facies. These deposits unconformably overlie bedrock strath which serves as a key geomorphic marker when exposed at the base of the terrace deposits. The alluvial deposits underlying fluvial terrace treads contain subangular to rounded gravel of Piedmont provenance, variably mixed with stratified sand, silt, and clay. The gravel is smooth, and locally polished, with respect to the quartz lags found in the residual deposits.

*Lithostratigraphy*

The combination of textural and compositional analysis, and field observations of terrace morphology, stratigraphy, and pedogenic development resulted in the identification of five

major terraces (Figure 6) and allowed for deposit characterization on which terrace correlations were anchored. Large ranges in elevation above the current channel were observed for multiple terraces in the mapping area and preclude the assistance of deposits' relative elevation in terrace identification. Terrace elevations above the current channel are not reported.

**QTr**- Upland Residual Gravel Deposits: Large, flat benches thinly mantled with gravel derived from residual soils and alluvial deposits. Deposits are heterogeneous, containing colluviated vein quartz and angular to subangular quartzite cobbles. Quartzite clasts are primarily ferruginous with hard, iron-rich weathering rinds > 1mm in thickness. Infrequent Precambrian Antietam Quartzite clasts containing skolithos tubes presumably reworked from older dismembered alluvial deposits.

**Qt1**: Poorly-preserved upland terrace deposit with low concentrations of gravel due to a high degree of erosional stripping and colluvial reworking.  In some case only the bedrock strath and terrace morphology is preserved. The deposits are sometimes associated with Masada soil series and where preserved, are deeply weathered, clay-rich, and contain very coarse angular quartz sand grains, likely from in-situ weathering of metamorphosed vein quartz. With increasing depth in the soil profile, the clay becomes more micaceous and/or transitions into a micaceous schist saprolite. Deposits are < 0.5 m thick.

**Qt2**: Deposit consists of moderately-eroded and colluviated, sub-rounded to rounded alluvial gravel, overlain by thin, clay-rich, red colluvial soils.  Most of the deposit is sub-rounded to rounded polycrystalline quartz with white, ochre, and ferruginous quartzites. The deposits are associated with both Masada and Turbeville soil series. Deposits are < 1 m thick.

23

**Qt3**: Deposit consists of a clast-supported gravel bed containing large, sub-rounded to rounded, white to off-white polycrystalline quartz. Significant components of white and ochre quartzite are also present, which are weathered, stained, and range in color from white, to yellow, to ochre. Less than 1% of the clasts are ferruginous quartzite, and no iron staining is observed in any clasts composed of polycrystalline or bull vein quartz. The gravel bed at the base of Qt3 is ~0.5 *m* thick and is overlain by ~1-1.5 *m* of deeply weathered, reddish-orange, polygenetic, alluvial and colluvial soils containing sandy matrix-supported water-worn gravels (Figure 8). Deposits are ~ 1 – 3m thick, inclusive of intact alluvium and multiple layers of overlying colluvium. Approximate depositional age is ~350-440 ka (RA1).

**Qt4**: Deposit consists of pebbles, the majority of which are polycrystalline quartz with irregular, iron-rich rings and significant iron staining in cracks. White quartzite clasts are subangular, with >1mm ferruginous weathering rinds. The base of the deposit is a gravel bed ~0.5 m thick that is overlain by a clast-poor, sand-rich layer and then multiple layers of a matrix-supported colluvium containing gravel of residual and fluvial origin. Where exposed, the soils of this terrace are similar to those described for Qt3, but less developed. The polygenetic soils are lighter in color and are developed through the matrix-supported sandy colluvium. Deposits are ~ 1 – 3 m thick, inclusive of intact alluvium and overlying colluvium. Approximate depositional age is 65-75 ka (MH1 and CH1).

**Qt4i**: Deposit is characterized by a basal bed, <0.5 m thick, of large, angular to sub-rounded, water-worn, and very smooth cobbles comprised mostly of unfractured vein and polycrystalline vein quartz, and smaller amounts of friable white and ochre quartzite. No ferruginous quartzite is present. The deposits contain locally-sourced clasts, evidenced by

24

the angular granodiorite clasts at Virginia Vermiculite mine, and the large amounts of translucent vein quartz at the lower Roundabout Farm deposit (RA2). The gravels are clast-supported, have a heavily-gleyed, mica-rich sand-clay matrix, with lenses of medium-grained sand. Qt4i is generally associated with the Masada Soil Series. Terrace deposits are ~1 – 2 m thick. Approximate depositional age is ~ 60-80 ka (VA and RA2).

**Qt4ii**: Suite of two terraces, vertically spaced approximately 3m apart. Gravel of the upper terrace deposit are supported in a sand-loam matrix, and the deposit becomes increasingly gravel-rich with depth. Compositionally, the upper deposits are 50-60% polycrystalline vein quartz, which is highly fractured and contains significant iron staining. The deposits of the lower terrace consist of a <0.5 m thick bed of clast-supported gravels, overlain by sandy loam and silty overbank deposits. The lower terrace gravels are more than twice as large as the upper terrace and have lesser amounts of iron staining. There is little to no white quartzite present in either the upper or lower deposit. The soils in the Qt4ii deposit commonly, but not always, map into the Masada Series. These soils have yellow, brownish-yellow, and yellowish-red sandy loam B horizons developed through the overbank facies that transition to brownish red, more clay-rich B horizons developed in the gravelly facies.

**Qt5**: Lowest deposit above the modern flood plain downstream of the Yanceyville knickpoint. Thin deposits (< 0.3 m) generally cap knolls composed of a clast-supported layer. Texturally, the gravels are highly varied in size and compositionally are up to 80% polycrystalline vein quartz and vein quartz, with lesser amounts of white quartzite. Generally, no iron-stained or ferruginous quartzites are present. The gravel bed is usually

overlain by colluvium, and the soils developed in the colluvium are of deeply weathered, reddish-orange, polygenetic.

**Qal**- Holocene and modern unconsolidated alluvial materials: Clay, silt, sand, and gravel, including clasts both locally-derived from vein quartz and bedrock as well as rounded cobbles remobilized from older fluvial deposits. Alluvium proximal to the South Anna River frequently contains legacy fines resulting from the construction and maintenance of mill dams along the river in the nineteenth and twentieth centuries. < 2 m thick.

*Luminescence Dating*

The OSL/IRSL burial ages of sampled terraces are displayed in Table 1. Each layer of interest was sampled twice. Samples VA 05A and 05B were the only samples for which the quartz grains analyzed were not saturated, and therefore quartz OSL provided finite ages of $67.0 \pm 25.7$ and $69.2 \pm 16.4$ ka, respectively. These samples were collected at the Virginia Vermiculite Mine (38° 3' 20"N; 77° 8' 39") from a stone line (Qt4i) consisting of well-rounded, pebbles and cobbles, which immediately overlies a mafic saprolitic body, primarily composed of vermiculite.

Three samples, VA 02 and VA03A and VA 03B were collected from Qt3 at Roundabout Farm (37°57'34" N; 78°1'7" W; RA1 in Figure 4), and because of quartz saturation, pIR-IRSL on potassium feldspar grains was performed on samples VA 02 and VA 03A. VA 02 was collected from a red, very sandy clay lens directly above a micaceous, hard, red, clay, interpreted as structured saprolite (Figure 8). VA 03A was collected approximately 20 cm above VA 02, in a layer of increased clast-richness but a similar red, very sandy clay

matrix. The reported ages for VA 02 and VA 03A are 391.8 ± 44.3 ka and 212.3 ± 29.2 ka, consistent with their respective stratigraphic position.

Once sample (LUVA-R1) was collected across the South Anna River from Roundabout Farm (37°57'29" N; 78°0'41" W; RA2 in Figure 4). The sample was collected at ~1.2 m depth from thick, heavily gleyed sandy-clay deposit (Qt4i), which was thought to be stratigraphcally above a gravel bed. The hand-dug pit did not reach the gravel layer, but the extensive gravel layer was exposed a few meters away, where sampling was not feasible. The reported pIR-IRSL$_{225}$ age is 81.5 ± 14.4 ka. One sample (LUVA-T1) was collected near the confluence of the South Anna River and Northeast Creek (37°56'4" N; 77°57'39" W; MH1 in Figure 4). The sample was collected at a depth of ~1.15m from a clast-rich sandy clay layer. The reported pIR-IRSL$_{225}$ age is 64.5 ± 8.7 ka.

Two samples, VA 04A and 04B were collected at a location on Chapman Farm (37°53'11"N; 77°55'15"W; CH1 on Figure 4) from a clast-rich layer (Qt4) of sandy red clay with subrounded to rounded pebbles overlying a red hard clay, interpreted as saprolite. The sampled layer was overlain by at least three distinct layers of colluvium. The IRSL age of sample VA 04 A is 73.5 ± 8.1 ka. Sample VA 04A was collected at ~1.1 m depth, and VA 04B, was sampled at ~1.0 m depth, and resulted in a pIR-IRSL age of 65.5 ± 8.1 ka. The sample was collected at a depth of ~1.1 m (Qt4) and rendered a pIR-IRSL$_{225}$ age is 64.5 ± 8.7 ka. One sample (LUVA-C1) was collected from Chapman Farm (37°56'4" N; 77°57'39" W; CH2 in Figure 4). The sample was collected at ~0.6m depth in a thick gravel layer (Qt4ii) overlying a hard clay, interpreted as saprolite. The sample has a reported pIR-IRSL$_{225}$ age is 200 ka, but is saturated and likely contaminated with saprolitic material.

Much of this thesis' work was accomplished by the collaboration and mentorship of USGS personnel. The USGS also collected samples for luminescence dating and have been kind enough to share the results of their samples, which are not included in Table 1, but will be incorporated in the discussion and overall geomorphic interpretation. The last round of OSL samples collected by the USGS are samples collected from an extensive terrace (QT5i) deposit at Morgan Hill Farm near the confluence of the South Anna River and Northeast Creek (37°56'20"N; 77°57'47"W; Harrison et al., *in progress*). The layer from which the samples were collected was clast-supported and had a red, sandy-clay matrix. The two samples collected here resulted in quartz OSL ages of approximately 40-50ka (Harrison, *personal communication*).

*Knickpoint Celerity Modeling*

The celerity modeling approach used is advantageous, because it allows for the quantification of the basin parameters $K$ and $m$ and can be efficiently applied to various knickpoints to test their genetic relation. In this study, both avenues were explored, the results of which are displayed in Tables 2 and 3. Despite possible variation among the channels examined, the ranges of $K$ and $m$ values that appear to be most representative of the South Anna River, The Newfound River, and their tributaries are 3.17E-6 to 1.01E-5 and 0.42-0.36, respectively.

The model of the predominant 52m knickpoint consistently generated an $m$ value of 0.36 and $K$ values which ranged from 6.70E-06 to 2.01E-05. When the $K$ and $m$ values provided 2% misfit between the actual and modeled horizontal location of the knickpoint on the tributaries used in the modeling, which is indicative of the knickpoints' genetic relation (Table 2a). When the various combinations of $K$ and $m$ values were applied to the

independent drainage basin of the Newfound River and the main trunk of the South Anna River, all of the combinations of $K$ and $m$ predicted the actual 52 m knickpoint location (at the given time) within 5% and 10%, respectively (Table 2b). This suggests the genetic relationship of the observed 52m knickpoints along the three tributaries, Newfound River, and the South Anna River. The only $K$ and $m$ pairs that predicted a knickpoint migration duration that were within the biostratigraphic age range of the Choptank Formation were 1.01E-5 and 0.36, respectively (in bold; Table 2B).

The 75m Owens Creek model accurately and precisely predicted the horizontal location of the 75m knickpoint on the three tributaries, thus, supporting a genetic relationship between the knickpoints.  All the $K$ and $m$ values ($K$=3.91E-6 to 2.82E-6 and $m$=0.42) generated from the models were then applied to the Newfound River and the South Anna and produced misfits between the predicted and actual location of the 75m knickpoint (Table 3A) within 13% and 20% along the Newfound River and South Anna River, respectively. Only the $K$ and $m$ values of 3.17E-6 and 0.42, respectively, predicted the age of the Choptank formation within age-range uncertainties (in bold, Table 3B). The model $K$ and $m$ outputs of the 85m knickpoint did not accurately predict the 85m knickpoint's location on the South Anna (Table 3B). These $K$ and $m$ values also failed to predict a reasonable age of the Choptank Formation (time related to the 150m knickpoint's migration), likely due to the large $m$ value of 0.82 (Table 3B). The predicted ages would imply that the 150m knickpoint migrated through the South Anna drainage at the incredibly rapid rate of ~80-110 km/Ma.

Although some of the model-generated $K$ and $m$ values did not accurately predict the 75m and 85m knickpoint locations along the Newfound River and South Anna River (Table 3),

it is not clear if these mal-predictions reflect a lack of genetic relation, or variation along the channels. In contrast, when the model was applied to 65m knickpoint on three tributaries of Taylor Creek and 85m knickpoint on three tributaries of Cub Creek, both models failed to converge. Despite possible variation among the channels examined, the ranges of $K$ and $m$ values that appear to be most representative of the South Anna River, the Newfound River, and their tributaries are 3.17E-6 to 1.01E-5 and 0.42-0.36, respectively.

Knickpoint celerity modeling was used to predict the rate of horizontal migration of acute rapid incision and implied terrace diachroneity for a given drainage basin and channel network. Using the range of model outputs of $K$ and $m$ that satisfied the time constraints of the Choptank Formation, the average calculated rate of knickpoint retreat in the mapping area ranged from 7-14 km/Ma.

DISCUSSION

Previous to this study, the fluvial terraces of the central Virginia Piedmont were mapped qualitatively, because mapping efforts were primarily bedrock-focused (Hughes, 2012; Spears and Gilmer, 2012), and the alluvial deposit texture, stratigraphy, and pedogenic development were not explored in great detail. This study presents the litho- and chronostratigraphic framework that may be used to better understand terrace genesis in this region, but the unit descriptions presented may be subject to modification as more terrace deposits in central Virginia are described, mapped, and dated. Field and laboratory studies generated the lithostratigraphy, spatial extents, and elevations (both relative and absolute) of the deposits. These data were then integrated with OSL/IRSL burial dating methods and numeric knickpoint celerity modeling to better quantify the two-dimensional (horizontal and vertical) elements of fluvial incision and interpretation of the dominant processes in terrace genesis.

*Incision and Terrace Formation Mechanisms*

Before integrating the geochronological data to correlate terraces, it is wise to consider what knickpoint celerity modeling may reveal about the rate of horizontal migration of acute rapid incision and implied terrace diachroneity. By assimilating elevations and age data of the axial terrace deposits along a longitudinal valley profile of the South Anna River (Figure 9) one can better compare terrace locations, elevations, and age data (Table 4) with calculated horizontal knickpoint celerity rates (Table 5). Using the pairs of model outputs of $K$ and $m$ that satisfied the age constraints of the Choptank Formation, the calculated rate of knickpoint retreat in the mapping area ranged from 7-14 km/Ma. This rate appears to be slightly higher than one might expect for an area absent of active tectonics (Whittaker and

Boultan, 2012), but serves as a first-order estimate of knickpoint retreat in the mapping area.

The calculated rates of knickpoint migration and terrace time-transgression can also be used to support or refute working terrace correlations and genesis hypotheses (Table 5; Figure 9). If the observed terraces represented the relict profile abandoned by knickpoint retreat, the knickpoint celerity rate should be able to predict age differences of correlative terraces and correlative terrace-knickpoint pairs. Although the calculated celerity rates are relatively swift, when compared to the OSL/IRSL-derived age differences between deposits and correlative knickpoints, the modeled rates are an order of magnitude too slow to predict the age difference (Table 5). For example, one possible correlation is the deposit at the Virginia Vermiculite Mine (VA) with the ~112m (Trevillians) knickpoint just upstream (Figure 9). The age difference between the deposit and the modern knickpoint is ~69,000 ± 16,400. When the representative $K$ and $m$ pairs were applied to the South Anna River channel between VA and the ~112m knickpoint, the predicted age differences were ~2,640,000 (K=3.17E-6, m=0.42) and 2,590,000 (K=1.0-E-5, m=0.36). The retreat rate predicted by these models is ~7km/Ma (Table 5). The age difference predicted by celerity modeling is over an order of magnitude greater than the reported OSL age difference. This would indicate that the Late Pleistocene VA deposit is not a terrace of the relict profile left by the initial migration of the ~112m knickpoint, but instead likely represents an intermediate terrace that was abandoned through vertical incision **after** the knickpoint migrated through the area (Figure 10). The repeated mismatch (Table 5) between the model-predicted and reported age differences between terraces and knickpoints suggests

32

that the terraces, assuming the ages reflect fluvial deposition, do not reflect the pre-knickpoint relict profile, but possibly intermediate terraces (Figures 9 and 10).

Although the initial retreat and terrace abandonment by knickpoints do not appear to be the source of the Pleistocene terraces presented here, it is unclear if the modern knickpoints in the area reflect migration and are still retreating or if they are more stable, arrested on structural or local geologic asperities (Hickok 1933; Morisawa, 1962; Frankel et al., 2007, Gallen et al., 2013; Miller et al, 2013). The fact that multiple models of knickpoint celerity support a genetic relationship between the 52m found on Beech, Cedar, and Taylor Creeks, the Newfound River, and the South Anna River and 75m knickpoints found along tributaries of Owens Creek, would suggest that the knickpoints may experience ongoing migration (Rosenbloom and Anderson, 1994; Whipple and Tucker, 1999; Berlin and Anderson, 2007; Crosby and Whipple, 2006). Alternatively, the fact that two models failed to converge, and that many of the tributaries of the South Anna River in the mapping area lack knickpoints at consistent elevations suggest that the retreat of some knickpoints may have been perturbed along their migration, either by external uplift or minor differences in rock erodibilities (Wobus et al., 2006).

*Climate, Vertical Incision, and Terrace Abandonment*

Alternatively, terraces along the South Anna River may better represent spatially-uniform but temporally-unsteady vertical incision, possibly driven by high-amplitude, high frequency climate fluctuations of the Late Pleistocene (Mills, 2000; Molnar 2004; Ward et al., 2005; Hancock and Kirwan, 2007). Given the uncertainties in geochronological data and modeled temporal lags of valley abandonment (Hancock and Anderson, 2002) it is unwise to draw conclusions about specific climatic events or intervals that may have caused

the formation of the observed terraces (Ward et al., 2005). However, drawing from a large body of empirical (Bull, 1991; Wegmann and Pazzaglia, 2002; Fuller et al., 2009) and numerical studies (Hancock and Anderson) of fluvial responses to external climate forcing, one can contemplate how the periglacial South Anna River may have reacted to climate fluctuations. Climate can modulate discharge, sediment load, and sediment size, and the interplay between these parameters results in variability in effective stream power and channel insulation, which dictate either lateral planation of straths or vertical incision and strath abandonment (Gilbert, 1877; Bull, 1991; Mackin, 1937; Wegmann and Pazzaglia, 2002; Hancock and Anderson, 2002; Fuller et al., 2009).

Increases in sediment supply can cause a reduction in fluvial transport capability, leading to channel-armoring, aggradation, and strath planation (Gilbert 1877; Hancock and Anderson, 2002; Wegmann and Pazzaglia, 2002; Personius et al., 1993; Fuller et al., 2009). The OSL ages (Figure 9) from strath terrace alluvium represent the depositional age of the sediment, when the South Anna River was actively cutting straths laterally and depositing alluvial materials. The geochronological data, do not, however, necessarily correlate with glacial time periods, which in North America have been analogously linked to increases in both the amount of sediment and the average grain size (Hancock and Anderson, 2002; Baker, 1974; Bull, 1991; Howard, 1970; Ritter, 1967; Sinnock, 1981). Additionally, numerical studies by Hancock and Anderson (2002) demonstrate that onset of rapid vertical incision and terrace abandonment is not synchronous with the periods of maximum discharge or minimum sediment supply, but lags behind the two by several tens of thousands of years. The time lags presented in the Hancock and Anderson study (2002) also supports threshold conditions in fluvial systems, where planation and incision

processes are dictated by fluctuations in transport capacity of the river, rather than the amount of fluvial inputs. Consequently, incision responses in periglacial South Anna River may not correlate with maximum climate fluctuations, and slight differences in local sediment or discharge inputs may cause responses disparate to regional trends (Hancock and Anderson). These findings reinforce the admonition of interpreting terrace chronostratigraphy presented here as regional climate proxy.

Increasing erosion rates (Shakleton et al., 1984; Molnar and England, 1990; Zhang et al., 2001) and variability ($10^4$-$10^5$ year) in incision histories (Ward et al., 2005) have been proposed to be a result of increasing amplitude of Late Cenozoic glacial-interglacial cyclicity. Time-averaged incision rates (calculated using depositional age data and the elevational separation between the deposits and the South Anna River; Table 4) produce a trend of increasing fluvial incision rates through time that aligns with findings of other studies in the Appalachians (Ward et al., 2005). The oldest, Middle Pleistocene deposit (RA1; ~390 ka) produces a time-averaged incision rate of ~60m/Ma, which is only slightly faster than time-averaged rates for other rivers in the Appalachians (45m/Ma; Ward et al., 2005), while many incision rates calculated for the Late Pleistocene deposits are more than double this rate (Table 4). However, it is important to note is that time-averaged incision rates are calculated over time-intervals that have components of both protracted lateral planation, and rapid vertical incision (Wegmann and Pazzaglia, 2002; Hancock and Anderson, 2002; Fuller et al., 2009). Mills (2000) and Hancock and Anderson (2002) proposed that apparent Late Cenozoic acceleration of incision rates calculated from many terrace sequences in the Southeastern United States reflects a bias caused by averaging over longer time-intervals, and more periods of lateral planation, as terrace age increases.

It is still unclear if the trend of increasing incision rates along the South Anna and other Appalachian rivers reflect increasing climate variability of calculation bias.

*Fluvial Responses to Tectonics*

Although vertical incision is the favored model of terrace abandonment creating the Middle to Late Pleistocene terraces flanking the South Anna River, the complicated age-elevation relationships of terraces proximal to the 2011 Mineral earthquake epicenter (Figure 9) are still fully unresolved.  The South Anna River flows orthogonal to the relevant fault plane of the 2011 Mineral earthquake (moment, $M_0$ $5.7 \times 10^{17}$ N·m), which had a hypocenter depth of $7 \pm 2$ km (McNamara et al., 2014). Although the previously unknown fault does not have an observed surface rupture, swarms of aftershocks have illuminated the previously-unknown fault plane as striking N 36° E and dipping east-southeast at 49.5°. (McNamara et al. 2014) The Morgan Hill Farm terraces lie along strike with the 2011 Mineral epicenter (Figure 4), and although the MH1 (Qt4) terrace has an elevation above the current channel that matches that of RA1 (Qt3; ~25m) it is much younger than RA1. MH1 has a depositional age of $64.5 \pm 8.7$ ka, which is almost ten times younger than the Middle Pleistocene age of RA1 ($\sim 400 \pm \sim 50$ ka). The Late Pleistocene age is also consistent with a similar depositional age, ~50 ka reported at a nearby location (MH2; Harrison, *personal communication*), where the extent of the terrace deposit, the lack of higher local topography, the observed stratigraphy suggest a fluvial (rather than colluvial) depositional age of the sampled layer.

The 2011 Mineral seismic event is believed to have created 7cm of permanent vertical surface displacement (Walsh et al., 2014). Although this is almost unperceivable to humans, affected river channels will re-equilibrate and return to a graded profile by

adjusting effective discharge through incising (Schumm, 1969; Suzuki, 1982; Whipple et al. 2000), meandering (Weems, 1991), and/or forming channel bed forms (Kennedy, 1963). Additionally, in the area along strike with the 2011 Mineral epicenter, including the Morgan Hill Farm deposits, there is a paucity of Middle Pleistocene terraces (Qt3; Figure 9). Instead, at comparable elevations above the current channel there is an abundance of Late Pleistocene terraces, (Qt4ii) which are a suite of two terrace levels, characterized by both levels having sandy overbank facies, iron-stained gravels, and an absence of white quartzite clasts. These terraces may reflect responses of the South Anna to tectonic uplift, although it is uncertain if tectonic uplift occurred coincident with formation of the Qt4ii terraces or only post deposition.

One can suggest many reasons for the formation and concentration of the preserved terraces. Coincident tectonic uplift from the growing fold could cause the reduction in slope above the epicenter. The reduced slope would decrease the overall effective discharge (Chezy, 1775; Manning 1895) and possibly cause channel aggradation, insulation, and lateral planation of the terraces. Additionally, enhanced erosion and colluviation by collective uplift could provide the system with more sediment locally, augmenting planation. Furthermore, endogenic, complex responses of rivers have been empirically shown to create unsteady threshold conditions, and in the absence of external forcing, could be responsible for variability in vertical incision and terrace creation (Frankel at al., 2007; Womack and Schumm, 1977; Shepard and Schumm 1974). The abundance of terraces directly above a growing fold (Walsh et al., 2014; Berti et al., 2015) could be related adjustment by the South Anna River to external tectonic forcing and sediment supply as well as cycles of autogenic unsteadiness. Additionally, these cycles may have a climatic
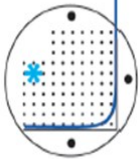
overprint, which, depending on the fluvial conditions present, may have diminished or enhanced terrace formation and preservation.

The rejection of knickpoint-related floodplain abandonment in favor of spatially-uniform vertical incision in the formation of the Pleistocene terraces supports correlative terraces having similar ages and occupying approximately the same elevation above the modern channel. Two terraces in our study that have similar ages are: sample VA, approximately 20 km upstream of the mapping area, which has an OSL age of ~ 69.2 ± 16.4 ka and ~16m of separation; and MH1 has an IRSL age of 65 ± 9 ka and ~25m of separation. The difference in their relative elevations above the modern South Anna River gives a rough estimate of the amount of uplift and/or enhanced vertical incision caused by movement of the fault associated with the 2011 Mineral earthquake. The ~10m difference between VA and RA1, over ~70ka would indicate that MH1 is experiencing ~0.1mm/year enhanced divergence from the modern channel. If we were attribute this divergence solely to co-seismic movement and assume ~7cm of permanent uplift per each 2011 Mineral-sized event (Walsh et al., 2014), it would take ~14 Mineral-sized events to create the observed separation. Over 70 ka, ~14 earthquakes could have a reoccurrence interval of ~1 earthquake per 5,000 years, consistent with an independent kinematic modeling of cumulative deformation (Malenda et al., 2014).

CONCLUSION

Two conceptual incision models are tested on terraces of the South Anna River to better understand the fluvial response to active tectonics in the Central Virginia Seismic Zone: 1) spatially-uniform vertical incision and 2) diachronous horizontal knickpoint retreat. Here, terraces and incision were evaluated in the context of a 1:24,000 scale surficial map of alluvial deposits, optically stimulated luminescence (OSL) and infrared luminescence (IRSL) geochronology, and knickpoint celerity modeling. Litho- and pedostratigraphically correlative deposits are found to form five groups of terraces (Qt1-Qt5) with similar, but not exact relative elevations above modern channel. Within these groups, the terraces have similar OSL/IRSL ages that do not systematically decrease in age upstream towards knickpoint in the modern channel. Similarly, the modeled rate of knickpoint retreat through the South Anna channel of ~7-14km/Ma is too slow to explain the OSL/IRSL dates for any terrace group. Terrace formation by knickpoint migration and horizontal floodplain abandonment is rejected as a dominant process in terrace formation, in favor of more spatially-uniform vertical incision, possibly related to unsteady Pleistocene climate fluctuations (Shakleton et al., 1984; Molnar and England, 1990; Zhang et al., 2001). Terraces are therefore best correlated using their stratigraphy, deposit texture and composition, degree of pedogenic development, and depositional ages. Terraces proximal to the 2011 Mineral earthquake epicenter have complicated age-elevation relationships, which are best explained by external tectonic forcing and local uplift along the fault.

TABLES

| Profile Location | Latitude | Longitude | Lithostrati-graphy | Sample number | USU Number | Number of aliquots[1] | Dose Rate (Gy/ka) | De[2] ± 2σ | Age[3] ± 2σ | OSL/IRSL |
|---|---|---|---|---|---|---|---|---|---|---|
| VA | 38° 3' 20"N | 77° 8' 39" W | Qt4i | VA-05A | USU-1579 | 9 (48) | 0.93 ± 0.07 | 62.00 ± 22.76 | 67.0 ± 25.7 | OSL |
|  |  |  |  | VA-05B | USU-1580 | 25 (51) | 0.93 ± 0.07 | 64.74 ± 13.6 | 69.2 ± 16.4 | OSL |
| RA1 | 37°57'34" N | 78°1'7" W | Qt3 basal | VA-02 | USU-1574 | 19 (22) | 1.65 ± 0.10 | -- | 407.8 ± 55.3[4] | IRSL[50] |
|  |  |  |  |  |  | 14 (22) | 1.65 ± 0.10 | -- | 391.8 ± 44.3[4] | pIRSL[225] |
|  |  |  | Qt3 alluv. fill | VA-03A | USU-1575 | 5 (19) | 2.46 ± 0.18 | -- | 230.4 ± 91.6[4] | IRSL[50] |
|  |  |  |  |  |  | 18 (19) | 2.46 ± 0.18 | -- | 212.3 ± 29.2[4] | pIRSL[225] |
| RA2 | 37° 57' 29"N | 78° 0' 41" W | Qt4i | LUVA-R1 | USU-1908 | 3 (3) | -- | -- | 81.5 ± 14.4 | pIRIRSL[225] |
| MH1 | 37°56' 4" N | 77° 57' 39" W | Qt4 | LUVA-T1 | USU-1905 | 3 (3) | -- | -- | 64.5 ± 8.7 | pIRIRSL[225] |
| CH1 | 37°53'11"N | 77°55'15"W | Qt4 | VA-04A | USU-1577 | 15 (21) | 2.20 ± 0.13 | 162.3 ±10.4 | 73.5 ± 8.1 | pIRIRSL[225] |
|  |  |  |  | VA-04B | USU-1578 | 19(19) | 2.20 ± 0.13 | 143.99 ±11.95 | 65.5 ± 8.1 | pIRIRSL[225] |
| CH2 | 37° 52' 39" N | 77° 54' 28" W | Qt5 | LUVA-C1 | USU-1907 | 3 (3) | -- | -- | >200[5] | pIRIRSL[225] |

1 Number of aliquots used in age calculations and the number of aliquotes analyzed in paretheses

2 Equivalent does (De) calculated using the Central Age Model of Galbraith and Roberts (2012), except where noted otherwise. De Values not available for fading corrected IRSL ages.

3 Ages analysis using either the single-aliquot regenerative dose procedure of Murray and Wintle (2000) on 1-2mm small aliquots of quartz sand (OSL) of the post-infrared infrared luminescne (pIR-IRSL) protocol of Buylaert et al. (2009) on 1-2 mm small aliquots of feldspar sand termperature of stimulation given.

4 IRSL Ages corrected for fading following Auclair et al. (2003).

Table 1: Age results for VA Vermiculite Mine (VA), Roundabout Farm (RA1 and RA2), Morgan Hill (MH1), and Chapman Farm (CH1 and CH2) deposits.

**Table 2. Model outputs, predictions and misfits of the 52m knickpoint**

| A. Actual x of K.P. | Model Outputs 52m KP | | | Beech | | Cedar | | Taylor | |
|---|---|---|---|---|---|---|---|---|---|
| S Anna | time input | m | k | Predicted x | % Misfit | Predicted x | % Misfit | Predicted x | % Misfit |
| 44432 | 3,000,000 | 0.36 | 6.70E-06 | 19,989 | 0% | 33,428 | 1% | 39,390 | 1% |
| Beech Creek | 2,500,000 | 0.36 | 8.04E-06 | 19,532 | 2% | 33,428 | 1% | 38,849 | 2% |
| 19989 | 2,250,000 | 0.36 | 8.94E-06 | 19,989 | 0% | 33,332 | 1% | 38,632 | 2% |
| Cedar Creek | 2,000,000 | 0.36 | 1.01E-05 | 19,989 | 0% | 33,428 | 1% | 38,849 | 2% |
| 33139 | 1,750,000 | 0.36 | 1.15E-05 | 19,989 | 0% | 33,428 | 1% | 38,849 | 2% |
| Taylor Creek | 1,500,000 | 0.36 | 1.34E-05 | 19,989 | 0% | 33,428 | 0.87% | 38,849 | 2% |
| 39606 | 1,000,000 | 0.36 | 2.01E-05 | 19,989 | 0% | 33,428 | 0.87% | 38,849 | 2% |

| B. Actual x of K.P. | Model Outputs 52m KP | | | Newfound River 52 m KP | | S Anna 52 m KP | | S Anna 500 pt long profile | |
|---|---|---|---|---|---|---|---|---|---|
| | time input | m | k | Predicted x | % Misfit | Predicted x | % Misfit | Choptank age | in range? |
| S Anna 52m | 3,000,000 | 0.36 | 6.70E-06 | 23,231 | 4% | 40,047 | 10% | 18,842,859 | no |
| 44432 | 2,500,000 | 0.36 | 8.04E-06 | 23,109 | 4% | 40,047 | 10% | 15,703,581 | no |
| S Anna 150m | 2,250,000 | 0.36 | 8.94E-06 | 22,988 | 5% | 40,047 | 10% | 14,132,264 | no |
| 153236 | **2,000,000** | **0.36** | **1.01E-05** | **23,231** | **4%** | **40,047** | **10%** | **12,556,799** | **yes** |
| @ 11.5-13Ma | 1,750,000 | 0.36 | 1.15E-05 | 23,109 | 4% | 40,047 | 10% | 10,994,049 | no |
| Newfound River 52 m | 1,500,000 | 0.36 | 1.34E-05 | 23,109 | 4% | 40,047 | 10% | 9,419,966 | no |
| 24082 | 1,000,000 | 0.36 | 2.01E-05 | 23,231 | 4% | 40,047 | 10% | 6,281,417 | no |

Table 2: Knickpoint celerity modeling results for the 52m knickpoint along Beech, Cedar, and Taylor Creeks. A: Model includes output values for *K* and *m,* the predicted distances of knickpoint migration, and the misfits, when compared to the actual horizontal locations listed in the farthest left column. B: Misfits of migration prediction when the *K* and *m* outputs are applied to the South Anna River and the Newfound River, as well as the age prediction for the Choptank Formation.

Table 3. Model outputs, prediction, and misfits of the 75m and 85 m on Owens Creek

| A. Actual x of K.P. | Modeling Outputs Owens Creek 75m | | | Newfound River 75 m KP | | S Anna 500 pts 75 m KP | | | |
|---|---|---|---|---|---|---|---|---|---|
| | time input | m | k | Predicted x | % Misfit | Predicted x | % Misfit | Choptank age | in range? |
| Newfound River 75m | 900,000 | 0.42 | 3.91E-06 | 36,245 | 13% | 77,085 | 20% | 10,074,177 | no |
| 41597 | 950,000 | 0.42 | 3.71E-06 | 36,245 | 13% | 77,085 | 20% | 10,633,967 | no |
| S Anna 75m | 1,000,000 | 0.42 | 3.52E-06 | 36,245 | 13% | 77,085 | 20% | 11,192,704 | no |
| 96945 | **1,250,000** | **0.42** | **3.17E-06** | **36,245** | **13%** | **77,085** | **20%** | **12,437,900** | **yes** |
| -- | 1,500,000 | 0.42 | 2.82E-06 | 36,245 | 13% | 77,085 | 20% | 13,994,835 | no |
| B. Actual x of K.P. | Modeling Outputs Owens Creek 85m | | | Newfound River 85 m KP | | S Anna 500 pts 85m KP | | | |
| | time input | m | k | Predicted x | % Misfit | Predicted x | % Misfit | Choptank age | in range? |
| Newfound River 85m | 1,000,000 | 0.84 | 8.95E-09 | 45,367 | **1%** | 150,723 | 34% | 1,402,827 | no |
| 45976 | 1,250,000 | 0.84 | 7.16E-09 | 45,246 | **2%** | 150,723 | 34% | 1,753,338 | no |
| S Anna 85m | 1,500,000 | 0.84 | 5.97E-09 | 45,367 | **1%** | 150,723 | 34% | 2,102,830 | no |
| 112581 | 1,750,000 | 0.84 | 5.11E-09 | 45,246 | **2%** | 150,723 | 34% | 2,456,731 | no |
| -- | 2,000,000 | 0.84 | 4.47E-09 | 45,246 | **2%** | 150,723 | 34% | 2,808,478 | no |

Table 3: Knickpoint celerity modeling results for the 75m (A) and 85m (B) knickpoint on Owens Creek. Model includes output values for $K$ and $m$, the predicted horizontal distances of knickpoint migration, the misfits, when compared to the actual locations in the farthest left column, and the age predictions of the Choptank Formation.

| Table 4: Locations, elevations, and time-averaged incision rates of terraces sampled for OSL/IRSL | | | | | | | |
|---|---|---|---|---|---|---|---|
| Location | Sample Elevation (m) | River Elevation (m) | dz (m) | X Location on SA (m) | Burial Age | Uncertain-ties +/- | Time-averaged vert. incision (mm/year) |
| VA | 121 | 105 | 16 | 140069 | 69,200 | 16,400 | 0.23 |
| RA1 | 111.5 | 86.4 | 25 | 117821 | 391,800 | 44,300 | 0.06 |
| RA2 | 96.8 | 86.0 | 11 | 117507 | 81,500 | 14,400 | 0.13 |
| MH1 | 105 | 80.2 | 25 | 106540 | 64,500 | 8,700 | 0.38 |
| CH1 | 105 | 71.8 | 33 | 86172 | 73,500 | 8,100 | 0.45 |
| CH2 [S] | 93.5 | 71.2 | 22 | 85545 | >200 | -- | -- |
| Knickpoints | x location on SA | Elevation | Age | | | | |
| Trevillians | 142575 | ~112m | 0 | | | | |
| Byrd Mill | 125341 | ~92m | 0 | | | | |
| Yanceyville | 110613 | ~85m | 0 | | | | |

Table 4: Locations and elevations (both relative and absolute) of terraces along the South Anna River and their corresponding time-averaged vertical incision rates. Location and elevation data extracted from a 10m DEM from the USGS national elevation database. "S" superscript denotes saturation and interpreted mixing with saprolitic material. Time-averaged incision rates calculated by dividing the elevational separation between the deposit and the modern channel.

| | Outputs from Owens Creek 75m KP | | Outputs from 52m KP on Beech, Cedar, and Taylor Creeks | | OSL/IRSL Time difference |
|---|---|---|---|---|---|
| Correlation | Modeled time difference m= 0.42; K=3.17 E-06 | retreat rate (km/Ma) | Modeled time difference m= 0.36; K=1.01E-05 | retreat rate (km/Ma) | |
| RA1 to Trevillians | 356,495 | 7 | 336,197 | 7 | 69,200 ±16400 |
| VA to Trevillians | 2,642,743 | 9 | 2,591,114 | 10 | 391,800 ± 44,300 |
| RA1 to VA | 2,286,248 | 10 | 2,254,917 | 10 | 322,600 ± 60,700 |
| RA2 to Byrd Mill | 692,372 | 11 | 698,879 | 11 | 81,500 ±14,400 |
| MH1 to Byrd Mill | 1,579,371 | 12 | 1,605,571 | 12 | 64,500 ±8,700 |
| MH1 to Yanceyville | 319,200 | 13 | 327,791 | 12 | 64,500 ± 8,700 |

Table 5: Knickpoint retreat predictions using K & m outputs

Table 5: Comparison of reported (OSL/IRSL) age differences between deposits and knickpoint celerity predictions for time between deposits. If deposits represent the relict profile abandoned by knickpoint retreat, the modeled time differences should be similar to the OSL-IRSL derived time differences (far right).
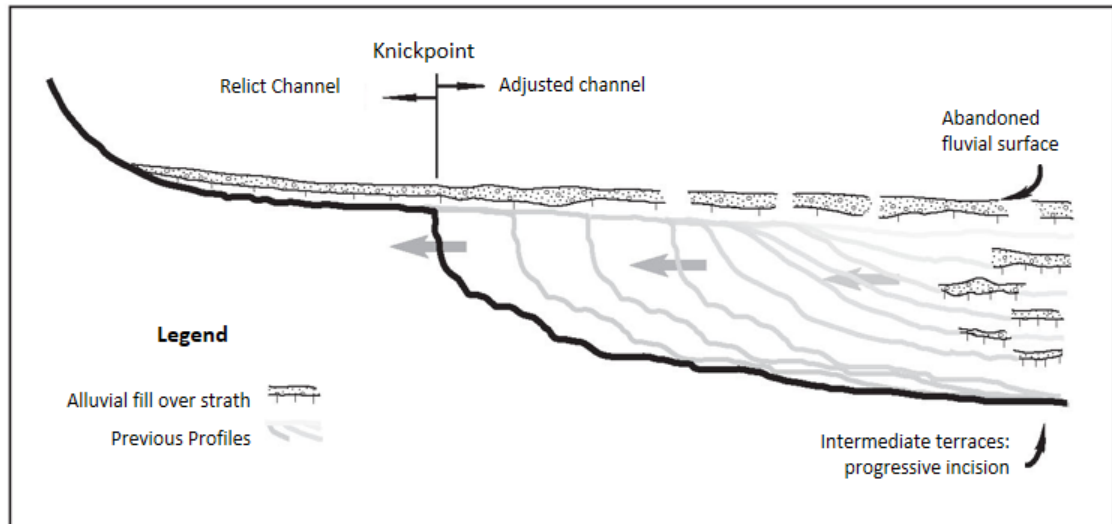
FIGURES



Figure 1: Cartoon of knickpoint migration, the formation of an adjusted river channel, abandoned profile, and intermediate terraces. The channel upstream is not yet impacted by the terrace and is therefore the "relict" profile (Crosby and Whipple, 2006).
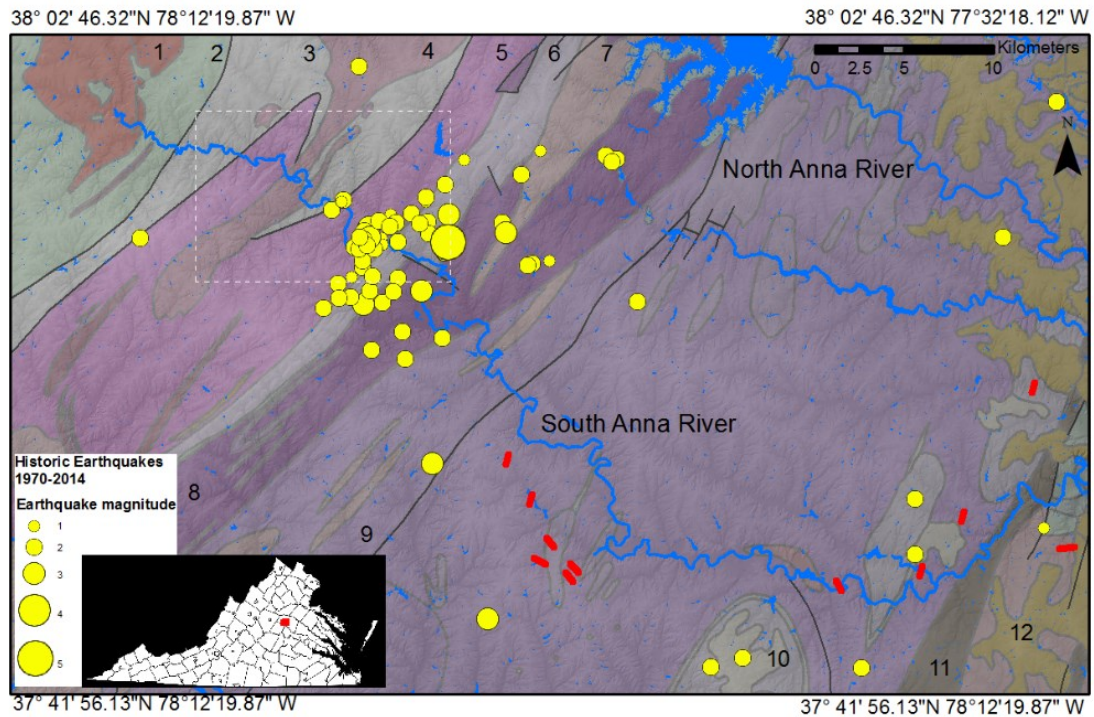
Figure 2: Map of study area with geologic overlay. White dashed line represents approximate area mapped as part of a USGS EDMAP study. Yellow circles indicate recent local earthquakes, which are scaled to magnitude (from the USGS). Red lines show knickpoints investigated in modeling. Geologic descriptions: 1) Proterozoic-Pennsylvanian Green Springs Pluton of diorite and hornblendite 2) Proterozoic-Cambrian meta-greywacke, quartzose schist and mélange 3) Ordovician Mine Run Complex, mélange zone III 4) Ordovician-Silurian Ellisville Biotite Granodiorite 5) Cambrian Chopawamsic Formation of interlayered felsic and mafic metavolcanic rocks 6) Ordovician Quantico Formation of slate and porphyroblastic schist 7) Mississippian-Pennsylvanian Falmouth Intrusive Suite of granite, quartz monzonite, granodiorite and tonalite 8) Cambrian Metamorphic Suite of Amphibolite gneiss 9) Proterozoic Porphyroblastic garnet-biotite gneiss 10) Proterozoic State Farm Hornblende-biotite granite gneiss 11) Proterozoic-Paleozoic mylonite gneiss, and cataclastic rocks 12) Miocene sand and gravel. Data from the USGS GIS database of geologic units and structures.
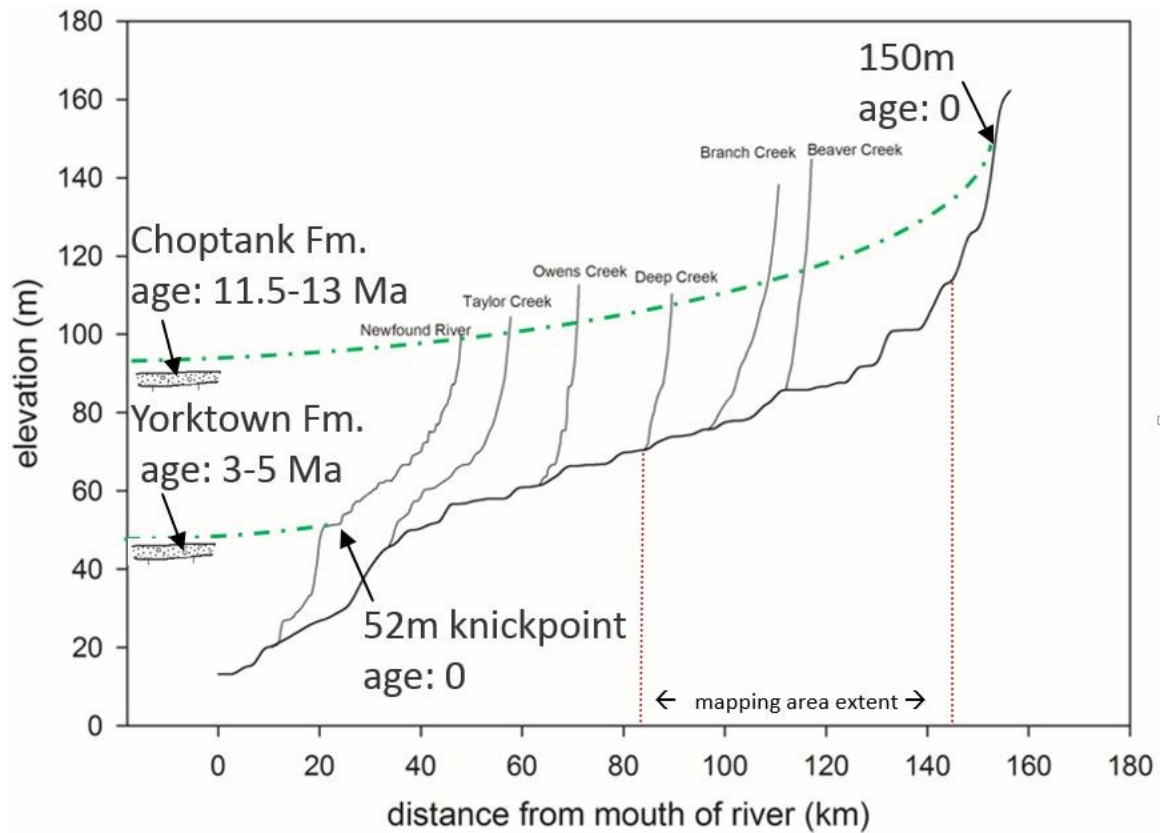
Figure 3: Longitudinal profiles of the South Anna River and major tributaries. Three tributaries with knickpoints at similar elevations are needed as inputs for the celerity model. Channel data from Newfound, Taylor, and Owens Creeks were used in knickpoint celerity modeling. Tributaries in the mapping area (Deep Creek, Branch Creek and Beaver Creek are shown here) had either anthropogenic and/or lacked knickpoints at consistent elevations, precluding their use in knickpoint modeling. Green lines show reconstructed paleo-profiles from the 150m knickpoint to the approximate elevation of the coastal Choptank Formation (top) and the 52m knickpoint to the elevation of the coastal Yorktown Formation (bottom). The age differences between the coastal deposits and their correlative knickpoints represent the time interval of knickpoint retreat.
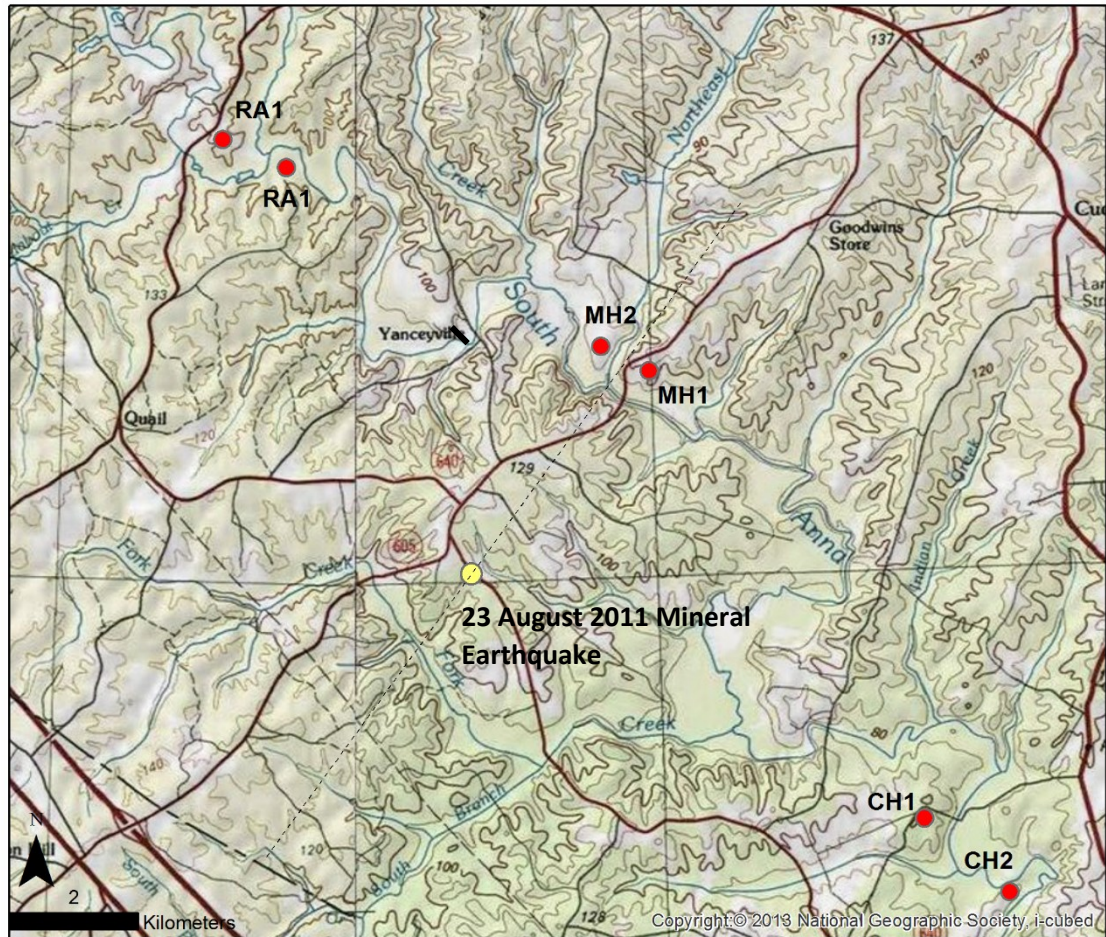
Figure 4: Approximate sampling locations for OSL/IRSL (in red). For scaling purposes, sample VA could not be shown on map (Sample VA is >20km upstream of Roundabout Farm; RA1 and RA2). Samples MH1 and MH2 are sampled near Morgan Hill Farm. Samples CH1 and CH2 were sampled from Chapman Farm. Yanceyville knickpoint shown with black bar. The approximate location of the 23 August 2011 Mineral earthquake epicenter is in yellow, and the relevant fault plane is shown with the dashed grey line. (McNamara et al., 2014)
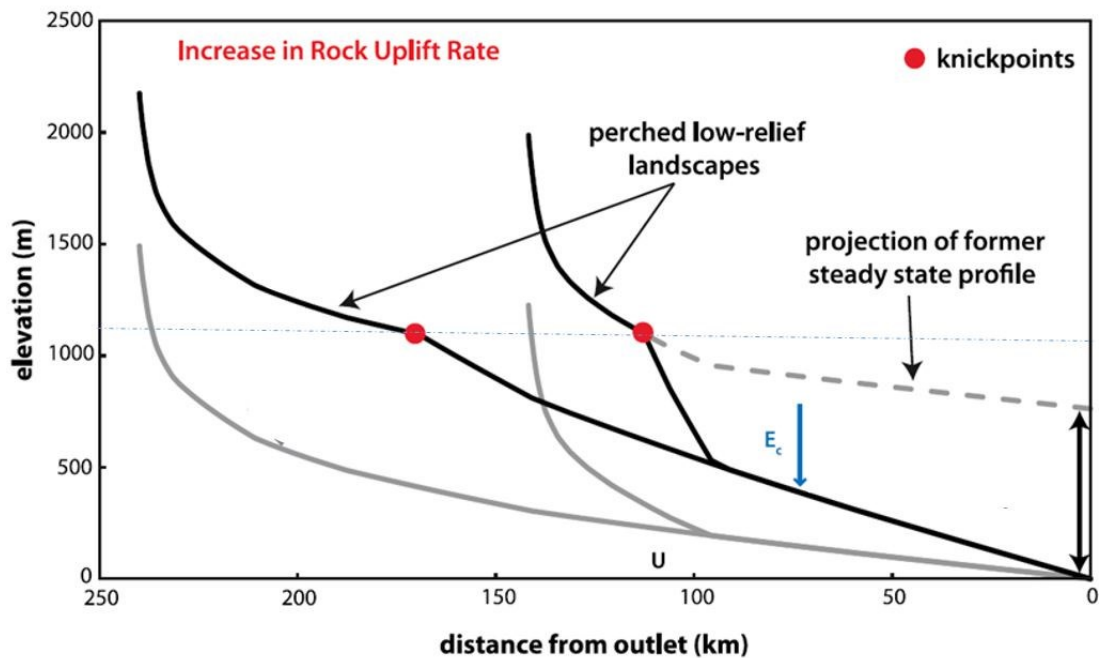
Figure 5: Cartoon depicting relative vertical and horizontal knickpoint migration (modified from Kirby and Whipple, 2012). Both black channels have experienced the same initial base-level fall (at the outlet). Horizontal migration is dictated by discharge and not congruent between the drainages, but due to scaling of local slope, vertical migration is constant, with both knickpoints occupying similar elevations (blue dashed line). Additionally, relict steady-state profile is shown in dashed grey line. Relict profile reconstruction is calculated using slope, concavity, and drainage area from the unadjusted channel upstream of the knickpoint (here, "perched low-relief landscapes").
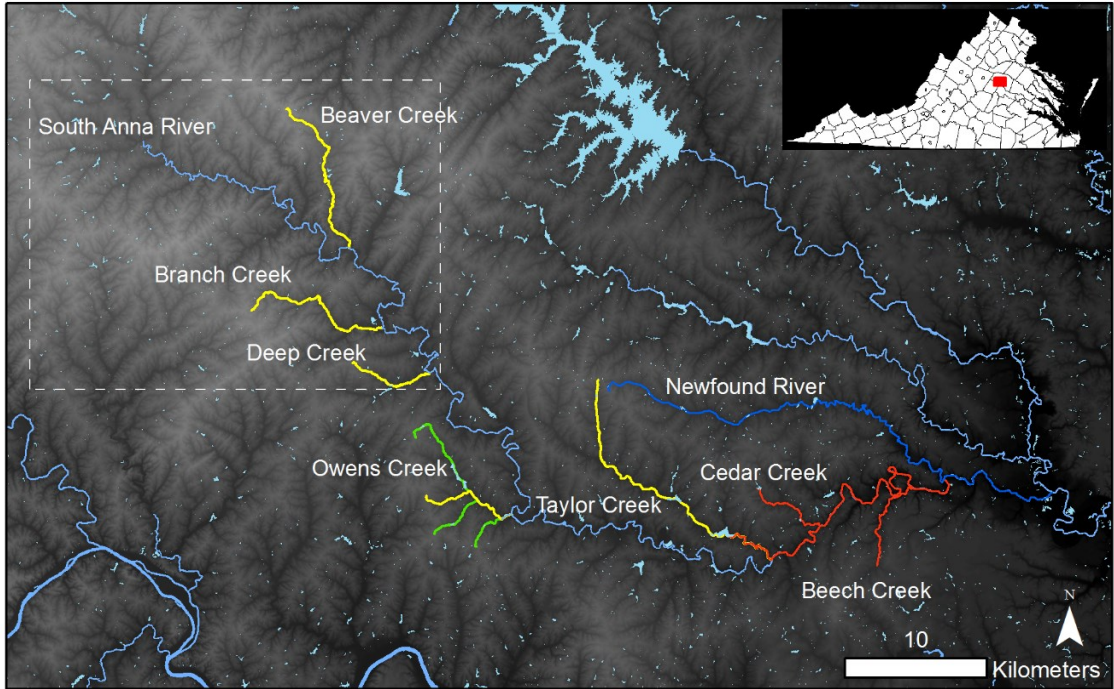
Figure 6: Ten meter digital elevation map (DEM) of the study area. Channels highlighted in yellow are included in the long profile in Figure 3, but not in the knickpoint celerity modeling. Channels highlighted in red are those used to model the 52 m knickpoint. The three tributaries of Owens Creek used to model the 75 and 85 m knickpoints are highlighted in green. The Newfound River (in blue) was used to as an independent drainage to assess the model-generated $K$ and $m$ values' ability to predict horizontal locations outside of the modeled drainage. White box outlines the approximate boundary of the mapping area.
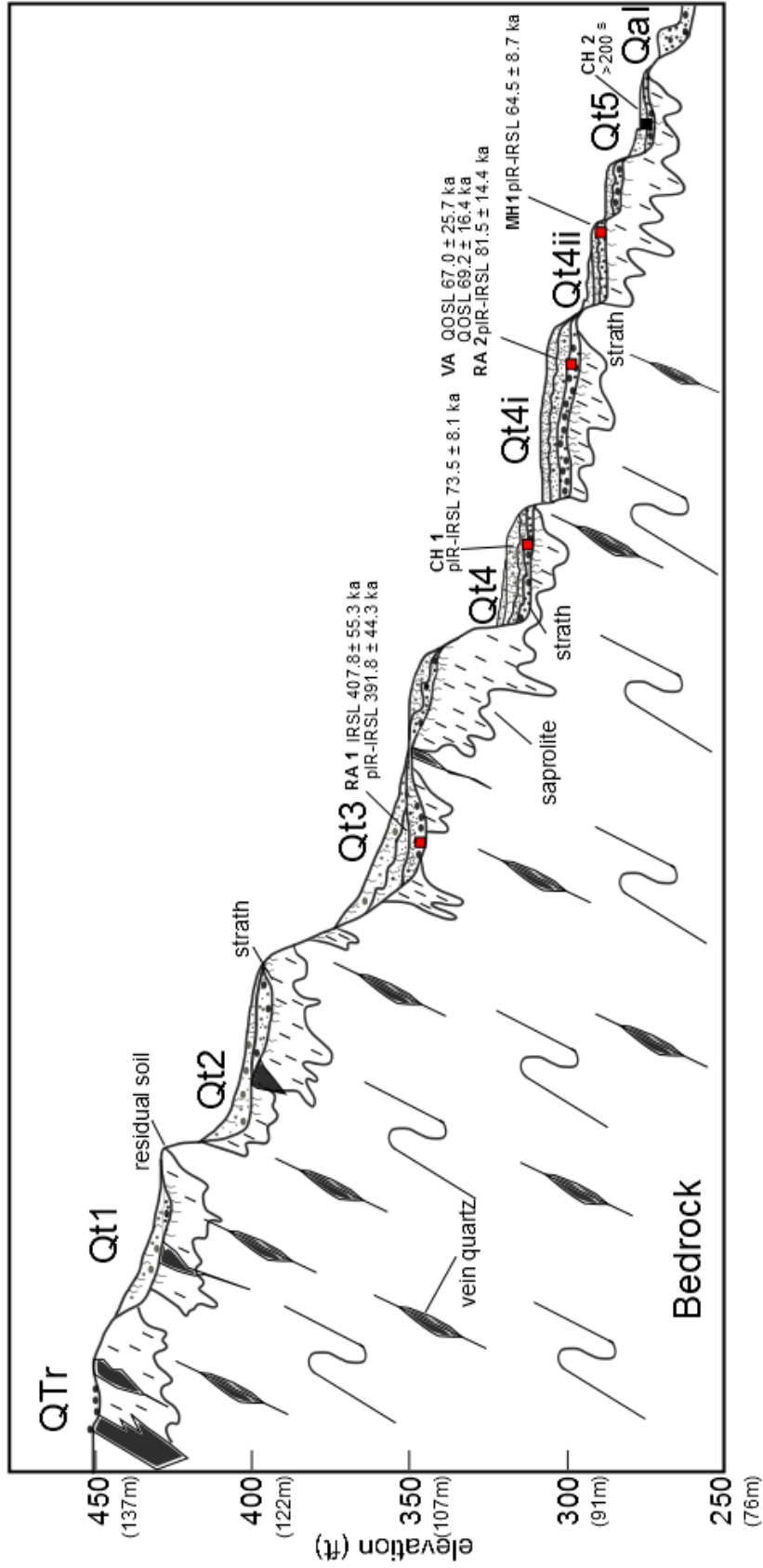
Figure 7: Schematic of the South Anna River lithostratigraphy of the Ferncliff, Pendleton, and northern quarter of the South Anna quadrangles, Virginia, USA (see appendix A for map deliverable). The half-valley cross section depicted here is a model compiled from the middle portion of the map area straddling the Ferncliff and Pendleton quadrangles. Locations of OSL/IRSL geochronology samples are show by the red boxes. Key relationships illustrated in this schematic include the genesis of straths and alluvial deposits in the modern valley bottom where there is a lack of saprolite and residual soil; formation of a fluvial terrace (Qt) following unsteady incision of the South Anna River; and significant colluviation of old alluvial deposits and residual materials developed in the Piedmont uplands.
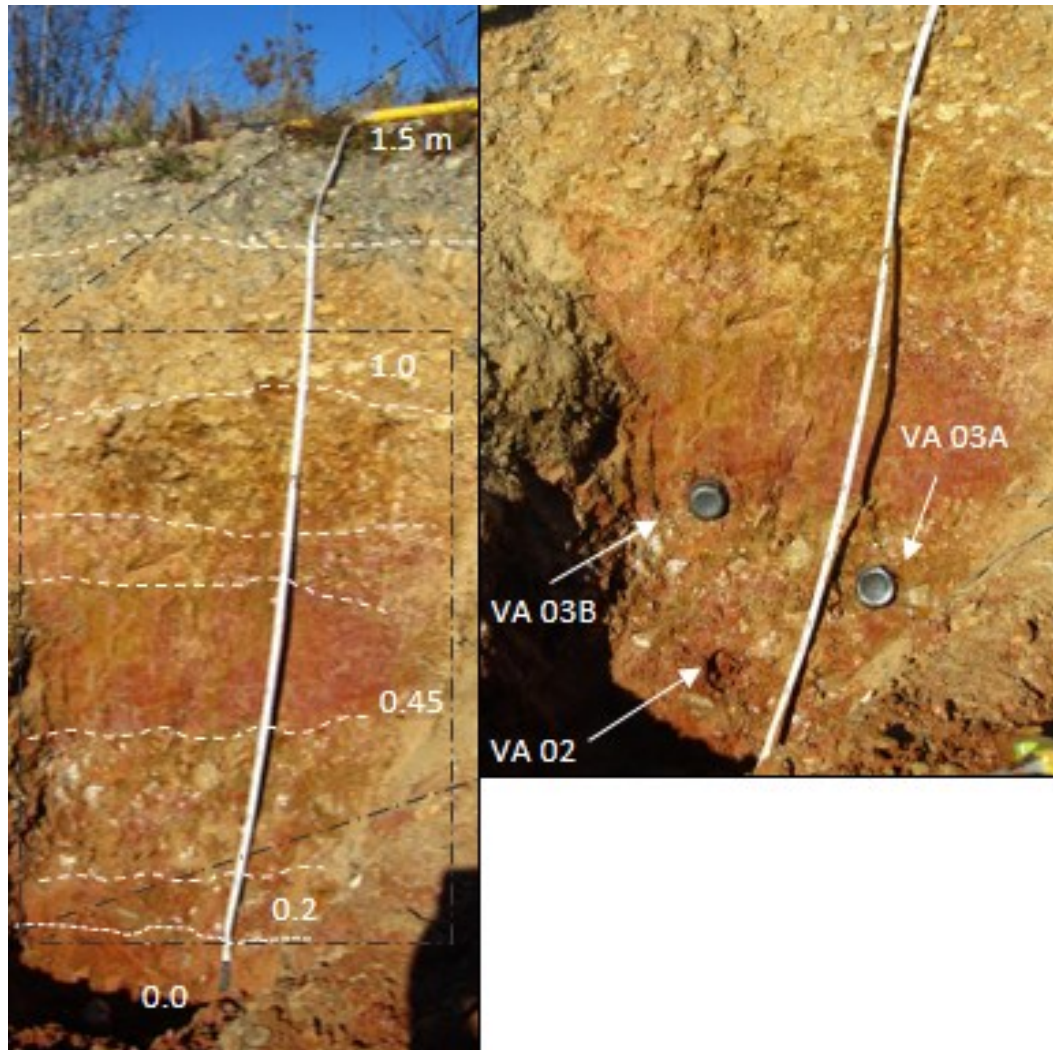
Figure 8: Vertical exposure of pit dug for OSL/IRSL sampling at Roundabout Farm (RA1; OSL/IRSL samples VA 02, VA03A, and VA 03B in Table 1). This photo shows a typical stratigraphy observed in surficial mapping project; at the base of the pit is structured or unstructured clay-rich saprolite, unconformably overlain by alluvial deposits of sandy-clay and rounded pebbles and gravels. Multiple colluvial wedges may cover the alluvial material, particularly in the older deposits, or deposits that do not occupy the highest local elevation.
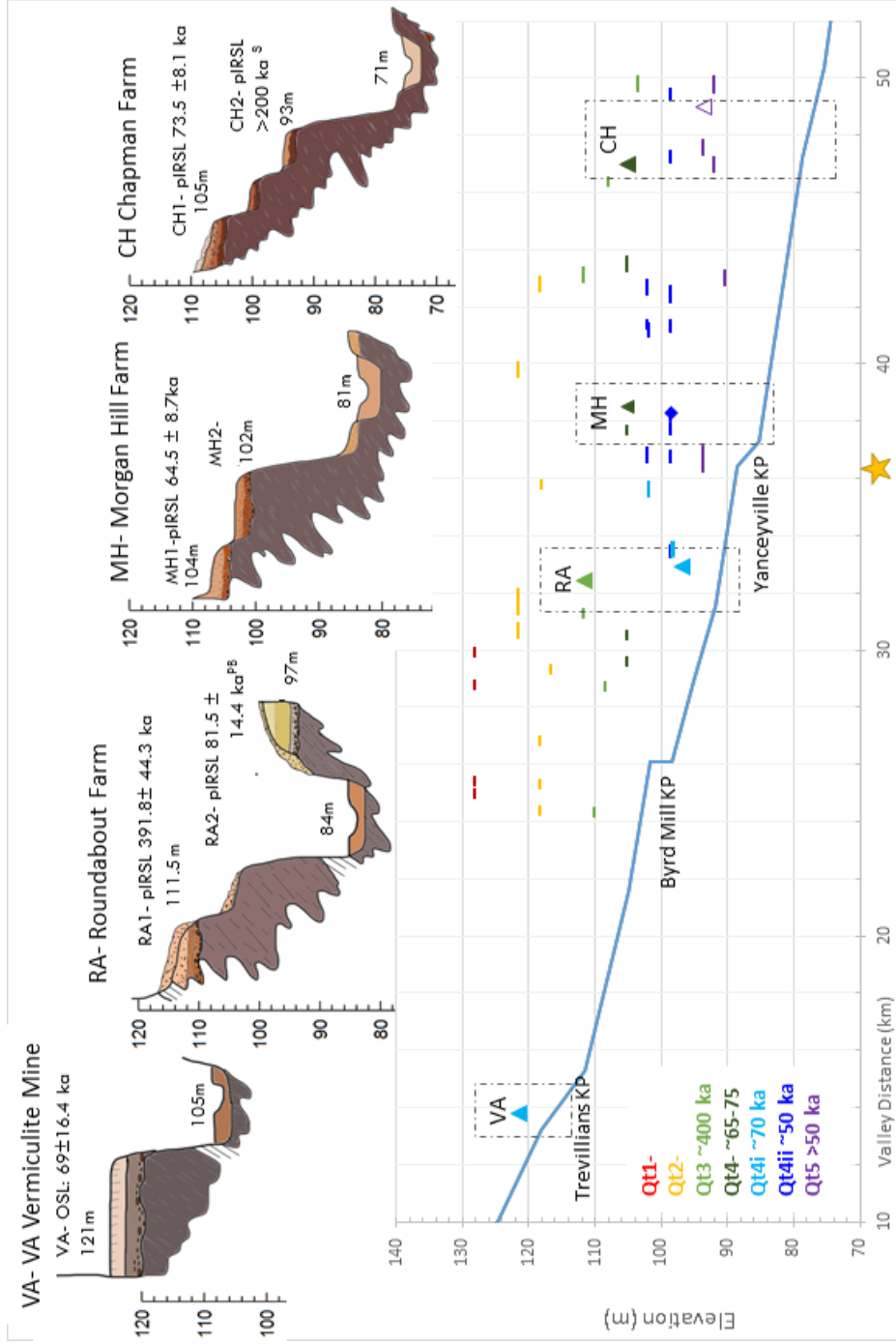
Figure 9: South Anna valley long profile with projected deposit elevation and interpreted terrace correlations. Axial terraces with strath elevations were projected perpendicularly onto the valley profile of the South Anna River (shown in blue). The colors of the terraces denote their assigned terrace unit (Qt). Closed Triangles: locations of OSL/IRSL sample collection with finite depositional ages Open triangle: location of OSL/IRSL sample with saturated age (likely due to saprolitic mixing). Closed diamond indicates site of the OSL sampling conducted by the USGS (Harrison, *in progress*). Yellow start indicates the approximate location of the 23 August 2011 Mineral earthquake, hypocenter not to scale (McNamara et al., 2014).
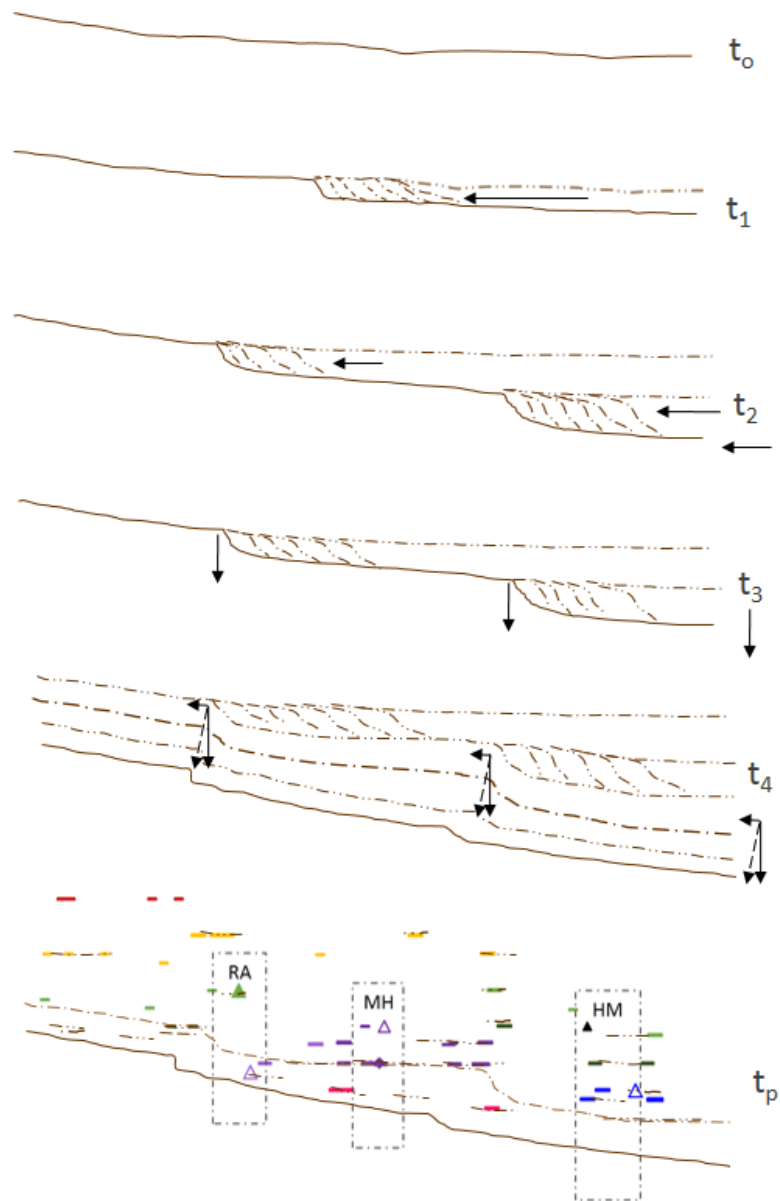
Figure 10: Cartoon sketch of conceptual model for terrace genesis. $T_o$ : Time before Byrd Mill knickpoint migration enters study area. $T_1$: Time of knickpoint migration associated with Byrd Mill. $T_2$: Time of migration associated with the Yanceyville knickpoint. $T_3$: Initiation of vertical incision becoming the dominant process in terrace genesis. $T_4$: Vertical incision is the dominant signal, possibly with a minor amount of horizontal knickpoint retreat. $T_p$: Present day. Valley long profile and deposit locations set behind conceptual distribution of terraces. Terraces do not necessarily represent pre-knickpoint relict profiles. Because of vertical incision, relict profiles (and associated terraces) appear higher than the knickpoints from which they were born.

REFERENCES

Aitken, M.J., 1998, An Introduction to Optical Dating: The Dating of Quaternary Sediments by the Use of Photon- Stimulated Luminescence: New York, Oxford University Press, 267 p.

Andrews, G. W. (1976). *Miocene marine diatoms from the Choptank formation, Calvert County, Maryland* (Vol. 910). US Govt. Print. Off..

Armbruster, J. G. and Seeber, L., 1987, The 23 April 1984 Martic earthquake and the Lancaster seismic zone in eastern Pennsylvania: Bulletin of the Seismological Society of America, v. 77, no. 3, p. 877-890.

Auclair, M., Lamothe, M., Huot, S., 2003. Measurement of anomalous fading for feldspar IRSL using SAR. Radiation Measurements 37, 487-492.

Baldwin, J. A., Whipple, K. X., & Tucker, G. E. (2003). Implications of the shear stress river incision model for the timescale of postorogenic decay of topography.*Journal of Geophysical Research: Solid Earth (1978–2012)*, *108*(B3).

Baker, V.R., 1974, Paleohydraulic interpretation of Quaternary alluvium near Golden, Colorado: Quaternary Research,v. 4, p. 94–112.

Berlin M., M., & Anderson, R., S., 2007, Modelling of knickpoint retreat in the roan plateau, western Colorado, J. Geophys. Res., 112, F03S06.

Berti, C., Pazzaglia, F. J., Meltzer, A. S., & Harrison, R. W., 2015, Evidence for persistent, cumulative deformation of the Virginia Piedmont in the vicinity of the 23 August, 2011 Mineral earthquake, in Horton, J. W., Chapman, M. C., and Green, R. A., eds., The August 23, 2011 Earthquake in Central Virginia and its Significance for Seismic Hazards in Eastern North America: Geological Society of America Special Paper, 509: 370-390.

Boettcher, S. S., & Milliken, K. L. (1994). Mesozoic-Cenozoic unroofing of the southern Appalachian Basin: Apatite fission track evidence from Middle Pennsylvanian s andstones. *The Journal of Geology*, 655-668.

Bouchard, M., Jolicoeur, S., & Pierre, G. (1995). Characteristics and significance of two pre-late-Wisconsinan weathering profiles (Adirondacks, USA and Miramichi Highlands, Canada). *Geomorphology*, *12*(1), 75-89.

Bull, W., 1991. Geomorphic Responses to Climate Change. *Climate Geomorphology.* Oxford University Press: London.

Bunte, K., & Abt, S. R. (2001). Sampling surface and subsurface particle-size distributions in wadable gravel-and cobble-bed streams for analyses in sediment transport, hydraulics, and streambed monitoring.

Burton, W.C., Harrison, R.W., Spears, D.B., Evans, N.H., and Mahan, S.A., 2015, Geologic framework and evidence for neotectonism in the epicentral area of the 2011 Mineral, Virginia, earthquake, *in* Horton, J.W., Jr., Chapman, M.C., and Green, R.A., eds., The 2011 Mineral,Virginia, Earthquake, and Its Signifi cance for Seismic Hazards in Eastern North America: Geological Society of America Special Paper 509, 331-341.

Buylaert, J.P., Murray, A.S., Thomsen, K.J., Jain, M., 2009. Testing the potential of an elevated temperature IRSL signal from K-feldspar. Radiation Measurements 44, 560-565.

Carter, M.W, Berquist, C.R., Bondurant, A.K., & Bleick, H.A. 2007 Geologic Map of the Bon Air Quadrangle, Virginia. Virginia Division of Mineral Resources Open File Report 07-03.

Chézy, A. (1896). DE, and M. Perronet: Unpublished report on the Yvette Canal.(1775) See Herschel, C. *J. Assoc. Engin. Soc*, *18*, 363.

Clark, G.M., and Ciolkosz, E.J., 1988, Periglacial geomorphology of the Appalachian Highlands and Interior Highlands south of the glacial border-A review: Geomorphology, v. 1, p. 191–220

Clark, G. M., & Hedges, J. 1992 "Origin of certain highelevation local broad uplands in the central appalachians south of the glacial border, USA: A paleoperiglacial hypothesis." *Periglacial Geomorphology, NewYourk: John wiley & Sons*: 31-61.

Crosby, B. T., and Whipple, K. X., 2006, Knickpoint initiation and distribution within fluvial networks: 236 waterfall in the Waipaoa River, North Island, New Zealand, Geomorphology, 82, 16-38.

Conrad, C. T., & Saunderson, H. C. 1999. Temporal and spatial variation in suspended sediment yields from eastern North America. *Geological Society, London, Special Publications*, *162*(1), 219-228.

Delcourt, H. R., & Delcourt, P. A. (1988). Quaternary landscape ecology: relevant scales in space and time. *Landscape Ecology*, *2*(1), 23-44.

Dowsett, H. J., & Cronin, T. M. (1990). High eustatic sea level during the middle Pliocene: Evidence from the southeastern US Atlantic Coastal Plain. *Geology*,*18*(5), 435-438.

Dowsett, H. J., & Wiggs, L. B. (1992). Planktonic foraminiferal assemblage of the Yorktown Formation, Virginia, USA. *Micropaleontology*, 75-86.

Eargle, D.H., 1997. Piedmont Pleistocene soils of the Spartenburg area, South Carolina: South Carolina Geology Notes, 21, 2, 57-74.

Ebel, J. E., 2009, Analysis of aftershock and foreshock activity in stable continental regions; implications for aftershock forecasting and the hazard of strong earthquakes: Seismological Research Letters, 80, 1062-1068

Faill, R. T. (1998), A geologic history of the north-central Appalachians. Part 3: The Alleghany orogeny, Am. J. Sci., 298, 131–179. Fischer, K. M. (2002), Waning buoyancy in the crustal roots of old mountains, Nature, 417, 933–936.

Flint, J.J., 1974. Stream gradient as a function of order, magnitude, and discharge. Water Resources Research 10, 969-973.

Frankel, K. L., Pazzaglia, F. J., & Vaughn, J. D. 2007. Knickpoint evolution in a vertically bedded substrate, upstream-dipping terraces, and Atlantic slope bedrock channels. *Geological Society of America Bulletin*, *119*(3-4), 476-486.

Fuller, T. K., Perg, L. A., Willenbring, J. K., & Lepper, K. 2009. Field evidence for climate-driven changes in sediment supply leading to strath terrace formation. Geology, 37(5), 467-470.

Galbraith, R. F., Roberts, R. G., Laslett, G. M., Yoshida, H., & Olley, J. M. 1999. Optical dating of single and multiple grains of quartz from jinmium rock shelter, northern Australia: Part I, experimental design and statistical models*.*Archaeometry*, *41*(2), 339-364.

Gallen, S. F., Wegmann, K. W., Frankel, K. L., Hughes, S., Lewis, R. Q., Lyons, N. & Witt, A. C. 2011 . Hillslope response to knickpoint migration in the Southern Appalachians: implications for the evolution of post-orogenic landscapes. Earth Surface Processes and Landforms, 36(9), 1254-1267Gardner, 1983

Gardner, T. W. 1983. Experimental study of knickpoint and longitudinal profile evolution in cohesive, homogeneous material. Geological Society of America Bulletin, 94(5), 664-672.

Gardneer, T.W., Jorgensen D. W., Schumm, C., & Lemieux, C. 1987. Geomorphic and tectonic process rates: effects of measured time interval. *Geology* 15, 259-261.

Gilbert, G.K., 1877, Geology of the Henry Mountains (Utah): Washington, D.C., U.S. Geographical and Geological Survey of the Rocky Mountains Region, 160 p.

Goldrick, G., & Bishop, P. (1995). Differentiating the roles of lithology and uplift in the steepening of bedrock river long profiles: an example from southeastern Australia. The Journal of Geology, 227-231.

Granger, D.E., Kirchner, J.W., and Finkel, R.C., 1997, Quaternary downcutting rate of the New River, Virginia, measured from differential decay of cosmogenic 26Al and 10Be in cave deposit alluvium: Geology, v. 25, p. 107–110.

Guerin, G., Mercier, N., Adamiec, G., 2011. Dose-rate conversion factors: update: Ancient TL 29, 5-8.

Hack, J. T. (1957). Studies of longitudinal stream profiles in Virginia and Maryland.

Hack, J.T., 1960, Interpretation of erosional topography in humid temperate regions: American Journal of Science, v. 258-A, p. 80–97.

Hack, J.T., 1973, Drainage adjustment in the Appalachians: in Morisawa, M. ed., Fluvial Geomorphology: Proceedings, 4th Annual Geomorphology Symposia, Binghamton, New York, 51-74.

Hack, M., 1975. "The Equality Problem for Vector Addition Systems is U Undecidable,"Computation Structures Group Memo 121, Project MAC, M.I.T. pp.l-32.

Hancock, G.,Kirwan,M., 2007. Summit erosion rates deduced from 10Be; implications for relief production in the Central Appalachians. Geology 35, 89–92.

Harkins, N., Kirby, E., Heimsath, A., Robinson, R., and Reiser, U., 2007, Transient fluvial incision in the headwaters of the Yellow River, northeastern Tibet, China: Journal of Geophysical Research, 112, doi:10:1029/2006JF000570.

Harris, L. D., de Witt, W., Jr., and Bayer, K. C., 1982, Interpretive seismic profile along Interstate 1-64 from the Valley and Ridge to the Coastal Plain in central Virginia: U.S. Geological Survey Oil and Gas Investigations Chart OC-123.

Hibbard, J. P., Van Staal, C. R., & Rankin, D. W. (2007). A comparative analysis of pre-Silurian crustal building blocks of the northern and the southern Appalachian orogen. *American Journal of Science*, *307*(1), 23-45.

Horton, J. W., Jr., Drake, A. A., Jr., and Rankin, D. W., 1989, Tectonostratigraphic terranes and their Paleozoic boundaries in the Central and Southern Appalachians, *in* Dallmeyer, R. D., editor, Terranes in the Circum-Atlantic Paleozoic Orogens: Geological Society of America Special Paper 230, p. 213–245.

Hatcher Jr, R. D. 1987. Tectonics of the southern and central Appalachian internides. *Annual Review of Earth and Planetary Sciences*, *15*, 337.

Hibbard, J. P., van Staal, C. R., and Rankin, D. W., 2007, A comparative analysis of pre-Silurian crustal "building blocks" of the northern and southern Appalachians: American Journal of Science, v. 307, n. 1,p . 23–45.

Hickok, W. O. 1933. Erosion surfaces in south-central Pennsylvania. American Journal of Science, (146), 101-122.

Howard, A.D., 1970, A study of process and history in desert landforms near the Henry Mountains, Utah [Ph.D. thesis]: Baltimore, Maryland, Johns Hopkins University, 361 p.

Howard, J.L. Amos, D.F., & Daniels, W.L. 1993. Alluvial soil chronosequence in the inner coastal plain, central Virginia: Quaternary Research, v. 39, p. 201-213.

Hughes, K. S., Hibbard, J. P., & Miller, B. V. (2013). Relationship between the Ellisville pluton and Chopawamsic fault: Establishment of significant Late Ordovician faulting in the Appalachian Piedmont of Virginia. *American Journal of Science*, *313*(6), 584-612.

Hughes, S., 2011. Geology of the northern half of the Ferncliff 7.5' quadrangle: U.S. Geological Survey EDMAP open file report, 313, scale 1:24,000.

Hughes, S., and Hibbard, J., 2012. Relict Paleozoic faults in the epicentral area of the August 23, 2011 Virginia earthquake; Geology in the Ferncliff, VA quadrangle: Geological Society of America Abstracts with Programs, v. 44, n. 4, p. 14.

Hughes, K. S., Hibbard, J. P., & Bohnenstiehl, D. R. (2015). Relict Paleozoic faults in the epicentral area of the 23 August 2011 central Virginia earthquake: Assessing the relationship between preexisting strain and modern seismicity.*Geological Society of America Special Papers*, *509*, 331-343.

Hulver, M.L., 1997, Post-orogenic evolution of the Appalachian mountain system and its foreland [Ph.D. dissertation]: Chicago, University of Chicago, 1055 p.

Huntley, D.J., Godfrey-Smith, D.I., and Thewalt, M.L.W., 1985, Optical dating of sediments: Nature, v. 313,p. 105–107.

Hütt G, Jaek I, Tchonka J. 1988. Optical dating: K-feldspars optical response stimulation spectra. *Quat. Sci. Rev.* 7:381–85.

Keller, M. R., Robinson, E. S, and Glover, L., III, 1985, Seismicity, seismic reflection, gravity, and geology of the central Virginia seismic zone: Part 3. Gravity: Geological Society of America Bulletin, v. 96, n. 12, p. 1580–1584.

Kennedy, J. F. (1963). The mechanics of dunes and antidunes in erodible-bed channels. Journal of Fluid Mechanics, 16(04), 521-544.

King, S.D., 2007. Hotspots and edge-driven convection. Geology 35,223–226.

Kirby, E., & Harkins, N. (2013). Distributed deformation around the eastern tip of the Kunlun fault. *International Journal of Earth Sciences*, *102*(7), 1759-1772.

Kirby, E., & Whipple, K. X. 2012. Expression of active tectonics in erosional landscapes. *Journal of Structural Geology*, *44*, 54-75.

Kochel, R.C., Eaton, L.S., Daniels, N., Howard, A.D., 1997. Impact of 1995 debris flows on geomorphic evolution of Blue Ridge debris fans, Madison County, Virginia (abstr.). Geological Society of America, Abstract with Programs 29 (6), 410.

Lampshire, L. D., Çoruh, C., & Costain, J. K. 1994. Crustal structures and the eastern extent of lower Paleozoic shelf strata within the central Appalachians: A seismic reflection interpretation. *Geological Society of America Bulletin*, *106*(1), 1-18.

Mackin, J. H. (1937). Erosional history of the Big Horn basin, Wyoming. Geological Society of America Bulletin, 48(6), 813-894.

Mackin, J.H., 1948. Concept of the graded river. Geological Society of America Bulletin 101, 1373–1388.

Malenda H.F., Pazzaglia, F.J., Berti, C., Nelson, M., Rittenour, T., Harrison, R. W., 2014. Investigating the presence of historical seismicity's effect on landscape evolution in the Central Virginia Seismic Zone, using fluvial stratigraphy and (paleo)geodesy [abs]: Geological Society of America- Annual Meeting inVancouver, British Columbia, Canada (19-23 October 2014) 272-14.

Manning, R., 1892. "On the flow of Water in Open Channels and Pipes." *Transactions Institute of Civil Engineers of Ireland,* vol. 20, pp 161-209, Dublin, 1891, Supplement, vol 24, pp. 179-207, 1895.

Matmon, A., Bierman, P. R., Larsen, J., Southworth, S., Pavich, M., & Caffee, M. (2003). Temporally and spatially uniform rates of erosion in the southern Appalachian Great Smoky Mountains. *Geology*, *31*(2), 155-158.

McNamara, D.E, Benz, H.M., Herrmann, R.B., Bergman, E.A., Earle, P., Meltzer, A., Withers, M., and Chapman, M., 2014, The M 5.8 Mineral, Virginia, earthquake of August 2011 and aftershock sequence: Constraints on earthquake source parameters and fault geometry: Bulletin of the Seism. Soc. of Am. 104, 1,. 40-54,.

Merritts, D. J., Vincent, K. R., & Wohl, E. E. (1994). Long river profiles, tectonism, and eustasy: a guide to interpreting fluvial terraces. *Journal of Geophysical Research: Solid Earth (1978–2012)*, *99*(B7), 14031-14050.

Mills, H.H., 1985, Descriptions of backhoe trenches dug on New River terraces between Radford and Pearisburg,Virginia, June 1981: U.S. Geological Survey Open-File Report 85-474, 63 p.

Miller, S. R., P. B. Sak, E. Kirby, and P. R. Bierman 2013. Neogene rejuvenation of central Appalachian topography: Evidence for differential rock uplift from stream profiles and erosion rates, Earth Planet. Sci. Lett., 369–370, 1–12

Mills, H. H., 1988, Surficial geology and geomorphology of the Mountain Lake area, Giles County, Virginia, including sedimentological studies of colluvium and boulder streams: U.S. Geological Survey Professional Paper 1469, 57 p.

Mills, H.H., 2000, Apparent increasing rates of stream incision in the eastern United States during the late Cenozoic: Geology, v. 28, p. 955–957

Mixon, R. B., Pavlides, L., Horton, J. W., Jr., Powars, D. S., and Schindler, J. S., 2005, Geologic map of the Stafford quadrangle, Stafford County, Virginia: U.S. Geological Survey Scientific Investigations Map 2841, scale 1:24,000.

Molnar, P., 2004, Late Cenozoic increase in accumulation rates of terrestrial sediment: How might climate change have affected erosion rates?: Annual Review of Earth and Planetary Sciences, v. 32, p. 67–89.

Mackin, J. H. (1937). Erosional history of the Big Horn basin, Wyoming. Geological Society of America Bulletin, 48(6), 813-894.

Moucha, R., Forte, A. M., Mitrovica, J. X., Rowley, D. B., Quéré, S., Simmons, N. A., & Grand, S. P. (2008). Dynamic topography and long-term sea-level variations: There is no such thing as a stable continental platform. *Earth and Planetary Science Letters*, *271*(1), 101-108.

Murray, A.S., and Wintle, A.G., 2000, Luminescence dating of quartz using an improved single-aliquot regenerative- dose protocol: Radiation Measurements, v. 32, p. 57–73.

Niemann, J. D., Gasparini, N. M., Tucker, G. E., & Bras, R. L. (2001). A quantitative evaluation of Playfair's law and its use in testing long-term stream erosion models. *Earth Surface Processes and Landforms*, *26*(12), 1317-1332.

Mixon, R. B., Pavlides, L., Powars, D. S., Froelich, A. J., Weems, R. E., Schindler, J. S., Newell, W. L., Edwards, L. E., and Ward, L. W., 2000, Geologic map of the Fredericksburg 30_ by 60 quadrangle, Virginia and Maryland: United States Geological Survey Geological Investigations Series Map I-2607, scale 1:100,000, 2 sheets.

Pagani, M. (2002). The alkenone-CO2 proxy and ancient atmospheric carbon dioxide. *Philosophical Transactions of the Royal Society of London. Series A: Mathematical, Physical and Engineering Sciences*, *360*(1793), 609-632.

Pavlides, L. (1989). Early Paleozoic composite mélange terrane, central Appalachian Piedmont, Virginia and Maryland; Its origin and tectonic history.*Geological Society of America Special Papers*, *228*, 135-194.

Pavlides, L. (1990). *Geology of part of the northern Virginia Piedmont*. U.S. Geological Survey report.

Pavlides, L. (1994). Early Paleozoic alkalic and calc-alkalic plutonism and associated contact metamorphism, central Virginia Piedmont.

Pavlides, L. (1995). Piedmont geology of the Stafford. *Storck, Salem Church, and Fredericksburg Quadrangles, Stafford, Fauquier, and Spotsylvania Counties, Virginia: US Geological Survey Open-File Report*, 95-577.

Pazzaglia, F. J., Gardner, T. W., & Merritts, D. J. (1998). Bedrock fluvial incision and longitudinal profile development over geologic time scales determined by fluvial terraces. *Rivers over rock: Fluvial processes in bedrock channels*, 207-235.

Pazzaglia, F. J., & Brandon, M. T. (1996). Macrogeomorphic evolution of the post-Triassic Appalachian mountains determined by deconvolution of the offshore basin sedimentary record. *Basin Research*, *8*(3), 255-278.

Pazzaglia, F. J., & Brandon, M. T. (2001). A fluvial record of long-term steady-state uplift and e erosion across the Cascadia forearc high, western Washington State. *American Journal of Science*, *301*(4-5), 385-431.

Pazzaglia, F. J., & Gardner, T. W. (1994). Late Cenozoic flexural deformation of the middle US Atlantic passive margin. *Journal of Geophysical Research: Solid Earth (1978–2012)*, *99*(B6), 12143-12157.

Pazzaglia, F. J. (2013). Fluvial terraces. *Treatise on geomorphology*, *9*, 37.

Peizhen, Z., Molnar, P., and Downs, W.R., 2001, Increased sedimentation rates and grain sizes 2–4 Myr ago due to the infl uence of climate change on erosion rates: Nature, v. 410, p. 891–897.

Personius, S. F., Kelsey, H. M., & Grabau, P. C. (1993). Evidence for regional stream aggradation in the central Oregon Coast Range during the Pleistocene-Holocene transition. *Quaternary Research*, *40*(3), 297-308.

Poag, C.W., and Sevon, W.D., 1989, A record of Appalachian denudation in postrift Mesozoic and Cenozoic sedimentary deposits of the U.S. middle Atlantic continental margin: Geomorphology, v. 2, p. 119–157

Pratt, T. L., Coruh, C., Costain, J. K., and Glover, L., III, 1988, A geophysical study of the Earth's crust in central Virginia: Implications for Appalachian crustal structure: Journal of Geophysical Research, v. 93, n. B6, p. 6649–6667.

Pratt, T. L., Horton, J. W., Spears, D. B., Gilmer, A. K., & McNamara, D. E. (2014). The 2011 Virginia Mw 5.8 earthquake: Insights from seismic reflection imaging into the influence of older structures on eastern US seismicity. *Geological Society of America Special Papers*, *509*, SPE509-16.

Prescott, J. R., & Hutton, J. T. (1994). Cosmic ray contributions to dose rates for luminescence and ESR dating: large depths and long-term time variations.*Radiation measurements*, *23*(2), 497-500.

Raup, C.J. 2014. Correlating River Terraces of the South Anna River with Photogrammetric Analysis of Clasts. Unpublished Senior Thesis, Lehigh University.

Regalla, C., Kirby, E., Fisher, D., & Bierman, P. (2013). Active forearc shortening in Tohoku, Japan: Constraints on fault geometry from erosion rates and fluvial longitudinal profiles. *Geomorphology*, *195*, 84-98.

Reusser, L. J., Bierman, P. R., Pavich, M. J. ,Zen, E., Larsen, J., Finkel, R. C., 2004. Rapid late Pleistocene incision of Atlantic passive-margin river gorges. Science 305, 499–502.

Rittenour, T. M., Goble, R. J., & Blum, M. D. (2005). Development of an OSL chronology for Late Pleistocene channel belts in the lower Mississippi valley, USA. *Quaternary Science Reviews*, *24*(23), 2539-2554.

Ritter, D.F., 1967, Terrace development along the front of the Beartooth Mountains, southern Montana: Geological Society of America Bulletin, v. 78, p. 467–484.

Rhodes, E. J. (2011). Optically stimulated luminescence dating of sediments over the past 200,000 years. *Annual Review of Earth and Planetary Sciences*, *39*, 461-488.

Rosenbloom, N. A., & Anderson, R. S. (1994). Hillslope and channel evolution in a marine terraced landscape, Santa Cruz, California. *Journal of Geophysical Research: Solid Earth (1978–2012)*, *99*(B7), 14013-14029.

Rowley, D. B., Forte, A. M., Moucha, R., Mitrovica, J. X., Simmons, N. A., & Grand, S. P. 2013. Dynamic topography change of the eastern United States since 3 million years ago. Science, 340(6140), 1560-1563.

Sasowsky, I. D., White, W. B., & Schmidt, V. A. (1995). Determination of stream-incision rate in the Appalachian plateaus by using cave-sediment magnetostratigraphy. *Geology*, *23*(5), 415-418.

Schumm, S. A., & Lichty, R. W. (1965). Time, space, and causality in geomorphology. *American Journal of Science*, *263*(2), 110-119.

Schumm, S. A. 1969. River metamorphosis. In *Journal of the hydraulics division, American society of civil engineers* (Vol. 95, No. HY1, pp. 255-273).

Schumm, S.A., and Rea, D.K., 1995, Sediment yield from disturbed earth systems: Geology, v. 23, p. 391–394

Seidl M.A. & Dietrich, W.E., 1992. The problem of channel erosion into bedrock. *Catena Suppl.* 23. 101-124

Shepherd, R. G., & Schumm, S. A. (1974). Experimental study of river incision. *Geological Society of America Bulletin*, *85*(2), 257-268.

Schoenbohm, L. M., Whipple, K. X., Burchfiel, B. C., & Chen, L. 2004. Geomorphic constraints on surface uplift, exhumation, and plateau growth in the Red River region, Yunnan Province, China. *Geological Society of America Bulletin*, *116*(7-8), 895-909.

Sinha, A. K., Thomas, W. A., Hatcher, R. D., Jr., and Harrison, T. M., 2012, Geodynamic evolution of the central Appalachian Orogen: Geochronology and compositional diversity of the magmatism from Ordovician through Devonian: American Journal of Science, v. 312, p. 907–966.

Sinnock, S. 1981. Pleistocene drainage changes in Uncompahgre Plateau-Grand Valley region of western Colorado, including formation and abandonment of Unaweep Canyon: A hypothesis. *NM Geol Soc Guideb*, *32*, 127-136.

Sklar, L., & Dietrich, W. E. (1998). River longitudinal profiles and bedrock incision models: Stream power and the influence of sediment supply. *Rivers over rock: fluvial processes in bedrock channels*, 237-260.

Snyder, N. P., Whipple, K. X., Tucker, G. E., and Merritts, D. J., 2000, Landscape response to tectonic forcing: Digital elevation model analysis of stream profiles in the Mendocino triple junction region, northern California, Geo. Soc. Of Am. Bull., 112, 1250-1263.

Spasojević, S., Liu, L., Gurnis, M., Müller, R. D., 2008. The case for dynamic subsidence of the U.S. east coast since the Eocene. Geophys. Res. Lett. 35, L08305.

Spears, D. B., and Bailey, C. M., 2002, Geology of the central Virginia Piedmont between the Arvonia synclineand the Spotsylvania high strain zone: 32nd Annual Virginia Field Conference, Charlottesville, Virginia, 36 p

Spears, D.B., Evans, N.H., and Gilmer, A.K., 2013, Geologic map of the Pendleton quadrangle, Virginia: U.S. Geological Survey Open-File EDMAP Map and Report, scale 1:24,000.

Spears, D. B., and Gilmer, A. K., 2012, Preliminary findings from recent geologic mapping in the central Virginia seismic zone: Geological Society of America Abstracts with Programs, v. 44, n. 7, p. 593.

Springer, G.S., Kite, J.S., and Schmidt,V.A., 1997, Cave sedimentation, genesis, and erosional history in the Cheat River Canyon,West Virginia: Geological Survey of America Bulletin, v. 109, p. 524–532.

Stein, S., and Liu, M., 2009, Long aftershock sequences within continents and implications for earthquake hazard assessment: Nature, v. 462, p. 87–89.

Suzuki, T., 1982, Rate of lateral planation by Iwaki River, Japan: Chikei (Transactions, Japanese Geomorphological Union), v. 3, p. 1–24.

Thomas, W. A., 2006, Tectonic inheritance at a continental margin, GSA Today, v. 16, p. 4-11.

van Staal, C. R., & Hatcher, R. D. (2010). Global setting of Ordovician orogenesis. *Geological Society of America Special Papers*, *466*, 1-11.

Vogt, P. R., 1991, Estuarine stream piracy: Calvert County, U.S. Atlantic coastal plain: Geology, v. 19, p. 754-757.

Wallinga, J., 2002, Optically stimulated luminescence dating of fluvial deposits: A review: Boreas, v. 31, p. 303–322.

Walsh, L. S., Montési, L. G., & Martin, A. J. (2014). Coulomb stress transfer and modeled permanent vertical surface deformation from the August 2011, Mineral, Virginia, earthquake. Geological Society of America Special Papers, 509, SPE509-18.

Walter, R. C., & Merritts, D. J. (2008). Natural streams and the legacy of water-powered mills. *Science*, *319*(5861), 299-304.

Ward, D.J., Spotila, J.A., Hancock, G.S., and Galbraith, J.M., 2005, New constraints on the late Cenozoic incision history of the New River, Virginia: Geomorphology, v. 72, p. 54–72.

Warrick, J. A., Rubin, D. M., Ruggiero, P., Harney, J. N., Draut, A. E., & Buscombe, D. (2009). Cobble Cam: Grain-size measurements of sand to boulder from digital photographs and autocorrelation analyses. *Earth Surface Processes and Landforms*, *34*(13), 1811-1821.

Watts, A. B., & Steckler, M. S. (1979). Subsidence and eustasy at the continental margin of eastern  North America. *Deep Drilling Results in the Atlantic Ocean: Continental Margins and Paleoenvironment*, 218-234.

Weems, R.E., 1988, Newly Recognized En Echelon Fall Lines in the Piedmont and Blue Ridge Provinces of North Carolina and Virginia, with a Discussion of their Possible Ages and Origin: U.S. Geological Survey Open-File Report 98-0374, 40 p.

Wegmann, K. W., & Pazzaglia, F. J. (2002). Holocene strath terraces, climate change, and active tectonics: The Clearwater River basin, Olympic Peninsula, Washington State. *Geological Society of America Bulletin*, *114*(6), 731-744.

Wehmiller, J. F., Belknap, D. F., Boutin, B. S., Mirecki, J. E., Rahaim, S. D., & York, L. L. (1988).  A review of the aminostratigraphy of Quaternary mollusks from United States Atlantic Coastal Plain sites. *Geological Society of America Special Papers*, *227*, 69-110.

Wheeler, R. L. and Bollinger, G. A., 1984, Seismicity and suspect terranes in the southeastern United States: Geology, v. 12, p. 323-326.

Whipple, K.X., 2001, Fluvial landscape response time: How plausible is steadystate denudation?: American Journal of Science, v. 301, p. 313–325.

Whipple, K., 2004. Bedrock rivers and the geomorphology of active orogens. Annual Review of Earth and Planetary Sciences 32, 151-185Whittaker and Boultan, 2012

Whipple, K. X., Tucker, G. E., 1999. Dynamics of the stream-power river incision model: implications for height limits of mountain ranges, landscape response timescales, and research needs. J. Geophys. Res. 104, 17661–17674.

Whittaker, A.C., Boulton, S.J., 2012. Tectonic and climatic controls on knickpoint retreat rates and landscape response times. J. Geophys. Res. 117, F02024.

Whittecar, G.R., Ryter, D.W., 1992. Boulder streams, debris fans, and Pleistocene climatic change  in the Blue Ridge Mountains of central Virginia. Journal of Geology 100, P. 487 – 494

Wobus, C., Whipple, K. X., Kirby, E., Snyder, N., Johnson, J., Spyropolou, K., Crosby, B., Sheehan, D., 2006 Tectonics from topography: procedures, promise, and pitfalls. In: Willett, S. D., Hovius, N., Brandon, M. T., Fisher, D. (Eds.), Tectonics, Climate, and      Landscape Evolution. Geo. Soc. Of Am. Boulder, Colorado, pp.55–74.

Wolin, E., Stein, S., Pazzaglia, F. J., Meltzer, A., Kafka, A., and Berti, C., 2012, Mineral, Virginia, earthquake illustrates seismicity of a passive-aggressive margin, Geophysical Research Letter, v. 39, L02305.

Womack, W. R., & Schumm, S. A. (1977). Terraces of Douglas Creek, northwestern Colorado: An example of episodic erosion. Geology, 5(2), 72-76.

Zaprowski, B. J., Evenson, E. B., Pazzaglia, F. J., & Epstein, J. B. (2001). Knickzone propagation in the Black Hills and northern High Plains: A different perspective on the late Cenozoic exhumation of the Laramide Rocky Mountains.*Geology*, *29*(6), 547-550.

APPENDICES

## *APPENDIX A: MAP*

Malenda, H. F., Raup, C.J., Pazzaglia, F.J., Berti, C., Harrison, R., Spears, D., 2014. Surficial map and geomorphic study of South Anna River Deposits, Virginia: Investigating the presence of ongoing and cumulative deformation in the Central Virginia Seismic Zone, Scale 1:24,000. USGS EDMAP Award: G13AC0015.

Map can be found at:
https://www.dropbox.com/s/5a2grs5x9fdserv/EDMAP_G13AC00115_For_release.pdf?dl=0

## *APPENDIX B: GRAVEL TEXTURAL ANALYSIS METHODS*

These methods are those developed and used by Cody Raup, which were included in his unpublished Senior Thesis (Raup, 2015)

Textural and compositional data for deposits were assembled to provide a quantitative and comparable basis for developing a lithostratigraphy and means of terrace correlation. Previous studies which investigated particle and particle-size distributions in fluvial settings (Bunte et al., 2001), as well as alternative photogrammetric approaches by the USGS (Warrick et al., 2009), set the framework for the compositional and textural analysis and the development of an efficient, software-based photogrammetric technique. The analyses were predicated on the assumptions that (1) the fluvial processes that transport gravels also round gravels, (2) gravel sourcing may have changed over time resulting in contrasting compositional distributions of the deposits (3) subsequent weathering of the deposits may create diagnostic weathering signatures such as weathering rinds. Textural parameters and compositional distributions were used in conjunction with relative weathering characteristics, pedogenic development, and soil stratigraphy (where possible) in deposit correlation.

Samples for textural and compositional analysis were collected from terrace alluvium. Gravel was collected at random from material removed from 1-1.75m pits dug into terrace treads or directly from deposits exposed at the surface. Sample selection bias was minimized by collecting all visible cobbles within a 1m2 area for the surface exposures, and by using a shovel and 5-gallon pail to take a grab sample for the pits and road cut exposures.

Splits of the field-collected cobbles were generated by randomly grabbing the first 100 clasts out of their 5-gallon containers. These clasts were thoroughly washed and dried.

The textural characteristics measured included gravel circularity (percent), roundness (percent), and size (area cm2). All of these metrics were analyzed computationally using the freely available program ImageJ (http://rsbweb.nih.gov/ij/). In this program circularity (C) is taken as a measure of how close an object is to a perfect circle, with 0%

being very elongated and 100% representing a perfect circle.  Computationally, this is expressed as

$$C = 4pA/(P)^2 \qquad\qquad (1),$$

where A is cross-sectional area (cm2), and P is perimeter (cm).  Similarly, roundness (R) is taken as a measure of angularity and surface roughness, with 0% being very angular and 100% being smooth and round.  This is expressed as:

$$R = 4A/(pXa)^2 \qquad\qquad (2),$$

where, Xa is the long axis (cm).

The clasts were carefully laid out on a 1-meter square white background such that none of their edges were in contact. A fluorescent bulb situated 1 m directly above the white background illuminated the samples while all other light sources were shut off. Using a tripod, the digital camera was situated in-line with the light source, so that no shadows were cast. To maximize contrast the picture was converted to a black and white image and was loaded onto ImageJ where scales and settings were adjusted to obtain a final analyzed image that reports the median, standard deviation, minimum, and maximum values for Xa, Xc (minor axis), A, P, R, and C.

Roundness and circularity, given in percentages, were analyzed non-parametrically by grouping the results of 16 samples (see appendix) into low (<70%), medium (70-75%) and high (>75%) categories. The clasts' areas, given in cm2 were compared, and those samples which had areas within 2 cm of one another were highlighted for further comparison. Once the clasts were analyzed for textural characteristics, they were broken open, sorted by lithology, and described. Characteristics that were noted included the friability of the quartzites, patinas, red and/or ochre staining, and the presence and thickness of iron-rich weathering rinds.

Terraces were characterized using the aforementioned suite of field observations and laboratory data, which included the deposits' morphology, texture, composition, provenance, pedogenic development, and elevation above local base level (see appendix for field and laboratory notes).

| Site # | Site Name | Latitude | Longitude | Elevation | Area (cm2) | Circularity (%) | Roundness (%) | White Quartzite | Ochre Quartzite | Ferruginous Quartzite | Vein Quartz | Polycrystalline Vein Quartz | Transluscent Quartzite | Intermediate Igneous |
|---|---|---|---|---|---|---|---|---|---|---|---|---|---|---|
| * | VA Vermiculite | 38°3'39"N | 77°8'39"W | 368 | 27.43 | 67% | 74% | 9% | 14% | 18% | 13% | 12% | 9% | 27% |
| 1 | Hicks | 37°59'20"N | 78°5'56"W | 360 | 10.07 | 76% | 69% | 12% | 16% | 6% | 3% | 63% | | |
| 2 | King Property | 37°57'44"N | 78°21'38"W | 420 | 22.91 | 64% | 75% | 20% | 13% | 42% | 6% | 19% | | |
| 3 | Round About Farm | 37°57'34"N | 78°1'7"W | 340 | 11.54 | 66% | 73% | 20% | 10% | 0% | 10% | 61% | | |
| 4 | Rodgers | 37°57'28"N | 77°0'35"W | 295 | 13.69 | 66% | 73% | 14% | 11% | 0% | 28% | 42% | 6% | |
| 5 | Badget Property | 37°56'45"N | 77°59'36"W | 312 | 13 | 73% | 71% | 9% | 5% | 0% | 32% | 48% | 7% | |
| 6a | Payne 300' | 37°56'36"N | 77°58'29"W | 300 | 10.6 | 78% | 72% | 1% | 10% | 18% | 23% | 48% | | |
| 6b | Payne Field | 37°56'33"N | 77°58'27"W | 310 | 3.3 | 75% | 76% | 0% | 13% | 30% | 5% | 52% | | |
| 7 | Thomas | 37°56'4"N | 77°57'39"W | 320 | 4.57 | 78% | 73% | 10% | 7% | 25% | 19% | 39% | | |
| 8 | Pebble Heaven | 37°55'19"N | 77°58'27"W | 310 | 4.36 | 79% | 72% | 9% | 9% | 0% | 18% | 65% | | |
| 9 | Hunters Hill | 37°54'8"N | 77°55'46"W | 360 | 7.94 | 75% | 75% | 20% | 2% | 23% | 14% | 40% | | |
| 10a | Cox Farm | 37°54'2"N | 77°55'51"W | 340 | 14.03 | 68% | 85% | 8% | 4% | 1% | 9% | 78% | | |
| 10b | Cox Island | 37°54'21"N | 77°56'34"W | 275 | 6.68 | 79% | 74% | 14% | 9% | 0% | 39% | 38% | | |
| 11 | Windy Knoll Farm | 37°54'6"N | 77°58'31"W | 350 | 19.89 | 65% | 72% | 0% | 6% | 8% | 3% | 83% | | |
| 12 | Harts Mill Road | 37°53'11"N | 77°55'15"W | 320 | 5.03 | 77% | 75% | 10% | 2% | 11% | 6% | 70% | | |
| 13a | Chapman Forest | 37°52'9"N | 77°54'57"W | 310 | 6.09 | 8% | 73% | 0% | 8% | 32% | 14% | 46% | | |
| 13b | Chapman Field | 37°52'39"N | 77°54'30"W | 285 | 9.98 | 79% | 73% | 16% | 2% | 0% | 38% | 43% | | |
| 14 | Horseshoe Farm (SA) | 37°58'17"N | 78°1'47"W | 290 | 4.78 | 77% | 72% | 7% | 7% | | 19% | 65% | | |
| 15 | RoundAbout Creek | 37°56'51"N | 78°2'49"W | 295 | 5.92 | 76% | 74% | 19% | | | 20% | 61% | | |
| 16 | Upland Hillslope | 37°57'50"N | 78°2'36" | 410 | 6.31 | 67% | 63% | | 3% | 3% | 61% | 33% | | |

Above: Examples of clast types for point count (from left to right) white quartzite, vein quartz, ochre quartzite, polycrystalline vein quartz., and ferruginous quartzite.

Below: Example of random clast collection for textural and compositional analysis.

Above: Examples of clasts from QTr.
Below: Example of Antietam quartzite with skolithos tubes found in QTr.

Above: Byrd Mill Knickpoint (~92m)
Below: Deposit at RA2 Site. Pit was filled in IRSL samples taken from silty
overbank deposits overlying the clast-rich layer.

Above: Bedrock strath outcrop of Qt1. Picture taken at Rollin Farm at the corner of Courthouse Rd (Rt 208) and Bickley Rd (Rt 642).
Below: VA Vermiculite Mine stone line from which OSL samples were collected

Above: Example of augering a terrace deposit for description of soil type.
Below: Morgan Hill (MH2) terrace tread. Minivan for scale.

## VA Vermiculite Mine (VA) OSL Samples VA05A AND VA05B



Clay-rich layer

Clay/verimiculite-rich layer

Stoneline

Mafic saprolite

Black-orange-green clays;

Black vitreous pockets, vermiculite pockets
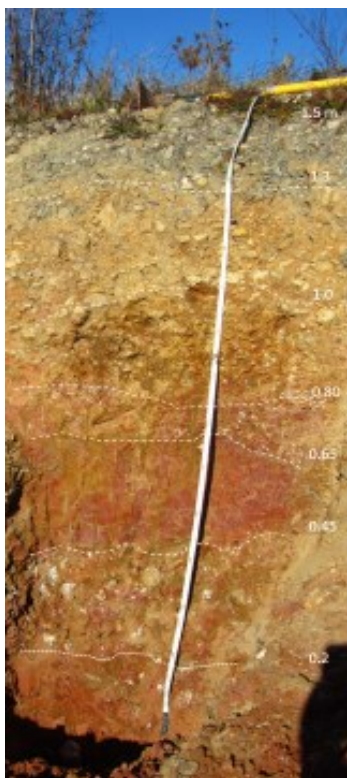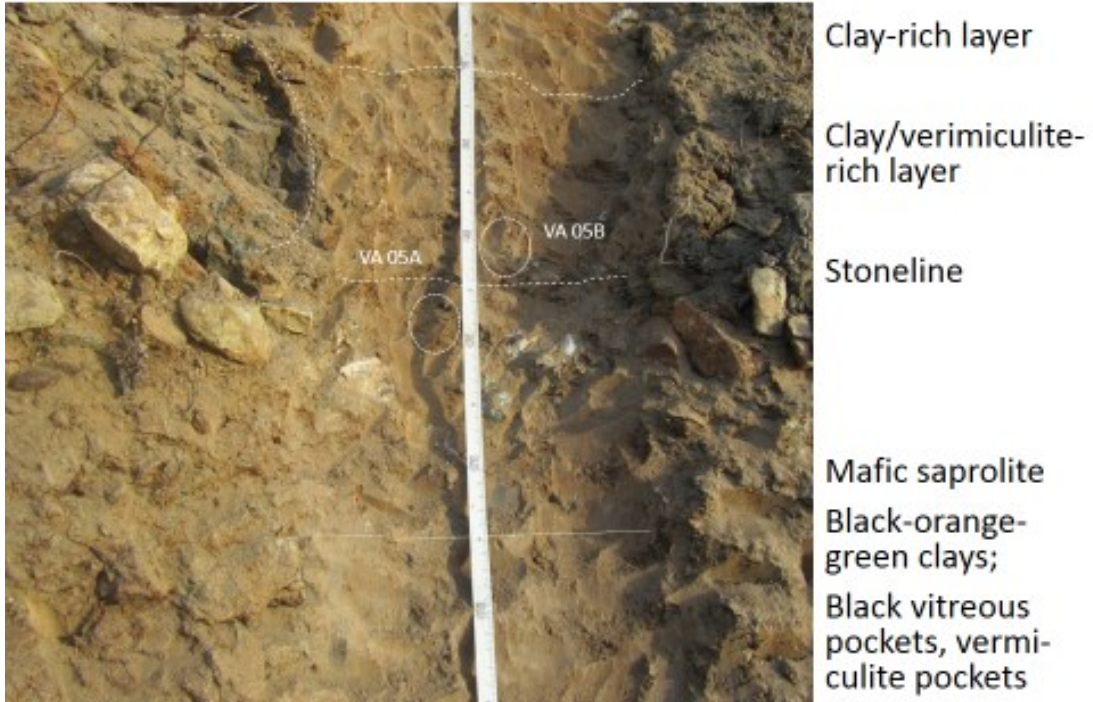
## Roundabout Upper (RA1)
## OSL Samples VA 02 &VA 03A/B



Disturbed grey-brown siltly organic matrix with subangular, clasts (2cm-5cm) 2.5 Y 7/2 (Roots)

Silty matrix- pebble rich, but matrix-supported, pebbles are subangular and 3cm-5cm 10 YR 7/2 (few roots)

Yellow clay being introduced, still silty, with smaller clasts 10 YR 6/6 (no roots)

Coarse Quartzite grains (</=0.5 cm) Red, white, yellow quartzite

Fine-course unstrat. Red, purple, orange sandy clay (Brick Red:10R 4/6 Purple-red: 7.5 R 3/6 Yellow: 7.5 YR 5/8

Finer sandy-clay matrix with subrounded cobbles 1-10 cm- becoming more clast-supported downsection

Micaceous, brick-red, hard clay; thought to be saprolite
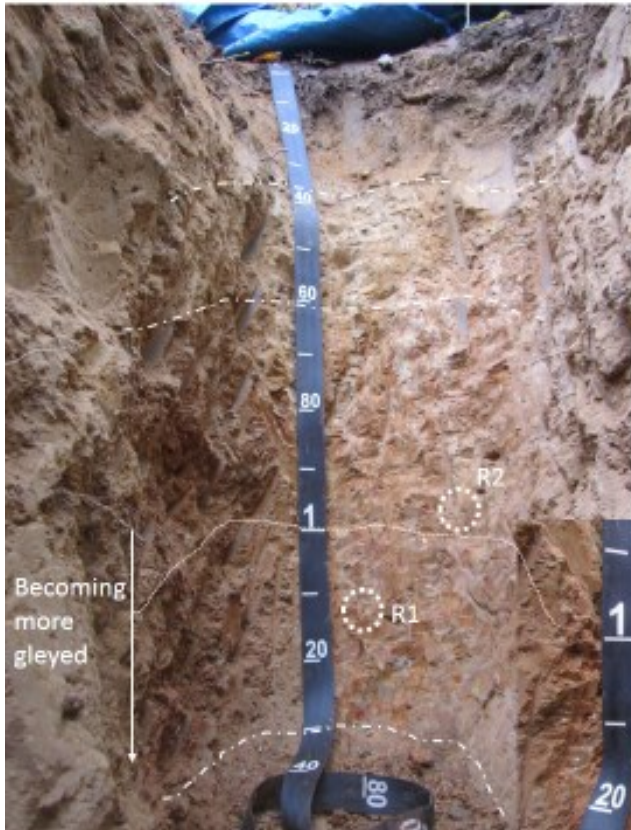
### Roundabout Lower (RA2)
OSL samples: LUVA R1 & R2
37 deg 57' 29 N; 78 deg 0' 41" W
Elevation: 315' 96.0 m
0.0-0.15m: O Horizon
0.15-0.4m: grey-tan (2.5YR 5/4)
    sandy loam with less roots
0.4-0.6m: yellow-tan (10YR 6/6)
    sandy clay, with small,
    angular pieces of qtz
0.6-1m: orange-brown (7.5 YR 5/8)
    sandy clay with angular,
    friable qtz; possible root
    structure white (2.5 YR 8/2)
    40 cm x 2cm
1-1.3m: sandy clay, more gleyed
    (10YR 6/2)

1.3M+ becoming redder with large clasts. Roots at bottom of pit.

Becoming more gleyed

### Morgan Hill Upper (MH1)
OSL Samples: LUVA T1&T2
37 deg 56' 4" N 77 deg 57' 39" W
Elevation 323' 98.5 m roots to bottom

0-0.4 m: red clay Fill
0.4-0.5m: grey-brown (10 YR 5/3) sandy loam
    (buried A)
0.5-0.8m: yellow-tan (10YR 6/6) sandy clay with
    pebbles and cobbles. Pebbles are rounded
    and Fe stained. Cobbles are angular.

0.8-1.0m: orange-brown (10YR 5/6) sandy clay
    less sand, <2 cm clasts with iron staining

1.0m-1.3m: sandy-clay layer becoming more clast-
    rich, many are well-rounded

1.3m+: Brick red clays
    (2.5 YR 4/8) with
    saprolite pieces into
    saprolite

Approx. location of DR
    collection
Roots present at the
    bottom of pit.

74

## Chapman Upper (CH1)
OSL Samples VA 04A/B

Grey-brown silty loam with mixed
clast sizes/roundness (2-8 cm; roots)

Matrix of grey-tan sandy silt.
Matrix-supported, subangular to
sub-rounded clasts (1-5 cm)
2.5 YR 5/4 (with fewer roots)

Very small (1-3cm) Qtzite pebbles
Red clay mixed in, with some sand

Clast-poor layer; Sandy clay
some small clasts mixing down-layer

Clast-rich layer in sandy red clay,
sub-rounded to rounded pebbles
(1-5 cm)

Right Tube not recovered.



## Chapman Lower (CH2)
OSL Samples LUVA C1
37 deg 52' 39"N -77 deg 54' 28"
Elevation: 286' 87 m
0.0-0.1m: organics red-brown
    (7.5 YR 4/6) clay loam
0.1-0.3m: orange-brown hard, plastic
    sandy clay with clasts below 0.2m
0.3-0.5: yellow and red mottling
            (10YR 6/8) and (2.5 YR 4/8)
0.5-0.8m: red-brown plastic clay
    with qtz clasts <1cm to >10cm
                Qtz is friable

0.8m+ brick red
clay, yellow
mottling (2.5 YR
4/8) no clasts
Foliation and
garnet and schist
pieces

Roots only to
clasts.

## APPENDIX F: Fortran Model

```
C

C
********************************************************************************
****

C   ***                                                                    ***

C   ***            PROGRAM KNICKPOINT                                      ***

C   ***               V. 4.0                                              ***

C   ***               FORTRAN                                             ***

C   ***                                                                    ***

C   ***     Frank J Pazzaglia, Claudio Berti, Jen Schmidt                  ***

C   ***               JANUARY, 2014                                        ***

C   ***                                                                    ***

C   *** This program will take a up to three long profiles, includ-
***

C   *** ing the area data and calculate the best-fit, min k and m          ***

C   *** values that satisfy the stream power equation. The user
***

C   *** specifies the range of k and m values to explore, as  well        ***

C   *** as the increment to step through the search. Output to the
***

C   *** screen is the minimum values.  The misfit to the data as a
***

C   *** function of k for the full range of m is written to an            ***

C   *** output file.                                                      ***

C   ***                                                                    ***

C
********************************************************************************
****

C
```

```
C

C    Just as a note to the user, place the distance of the knickpoint,

C    in meters, measured upstream from the mouth of the stream.

C    KP = knickpoint

C

C    KP1 = Owens4, 5772 m; KP2 = Owens2, 4629 m,

C    KP3 = Owens3, 4899 m

C


PROGRAM KNICKPOINT

C

     INTEGER H, I, J, C

     REAL X2(5000), XINC(5000), AINC(5000), MPRINT(1000, 1000)

     REAL KP3, KP2, KP1, KPAGE3, KPAGE2, KPAGE1, A

     REAL KSTART,KEND,KINC,MSTART,MEND,MINC

     REAL K, M, MFIT, KFIT, MISLOG, DIST

     REAL X1(5000), X3(5000)

     REAL A1(5000), A2(5000), A3(5000)

     REAL X1INC(5000), X2INC(5000), X3INC(5000)

     REAL X, XX(5000), DT, DT1, DT2, DT3, LOGCYCLE

     REAL KK, KKK, LCLOOP, KDYN, LOW, MISFIT

     CHARACTER*100 INFILE1, INFILE2, INFILE3

C

C

C    NOTE:  these knickpoint locations are hard-wired into the code

C    for the three streams being modeled. The code can be changed

C    to accommodate to ask for the knickpoint locations.

C

     KP1 = 5772

     KP2 = 4629

     KP3 = 4899

C

C

C    Here the user needs to indicate knickpoint age (KPAGE).  With

C    three streams, the user just supplies one knickpoint age for

C    KPAGE1 (in years).  In effect, KPAGE is usually a model age.

C

     KPAGE1 = 1500000

c    KPAGE2 = 6000000

c    KPAGE3 = 10000000

C

C

C    An output file is defined here to allow results to be written

C    to a text file for later plotting

C

     OPEN (UNIT=20,FILE='fitkm.csv')
```

```
C

C

C    The code here can be easily modified to uncomment these lines,

C    that allows the user to input these k parameters.  Otherwise, the

C    program will hard-code in these values. Of course, if there is to

C    be user input, that hard-coded values need to be commented out.

C

C     PRINT *, 'Please enter the starting k, ending k, and k-increment'

C     PRINT *, 'all separated by commas'

C     PRINT *, ' '

c     READ *, KSTART, KEND, KINC

C


      KSTART = 0.000000000001

      KEND =  0.0001

      LOGCYCLE = log10(kend/kstart)

C

C    Here, set the increment in k for a given log cycle. A kinc of 1

C    will result in 10 k values for one log cycle. A kinc of 0.1 will

C    result in 100 k values for one log cycle

C

      KINC = 0.001

C

C

C    This block of code allows the user to enter the m-value space to

C    be explored. As above, the input questions should be commented out

C    if the hard-coded values below are to be used instead.

C

C     PRINT *, ' '

C     PRINT *, 'Please ender the starting m, ending m and m-increment'

C     PRINT *, 'all separated by commas'

C     PRINT *, ' '

C     READ *, MSTART, MEND, MINC

C

      MSTART = 0.1

      MEND = 1

      MINC = 0.02

C

C

C    This block of code allows the user to enter the names of the

C    files containing the long profiles of the three rivers to be

C    analyzed.  Alternatively, the user can choose to comment out

C    the input instructions and simply hard-code in the names of

C    the long profiles in the OPEN statements below.

C

      PRINT *,' '

C
```

```fortran
C     PRINT *,'Please enter the names of 3-
column, comma-delimited'

C     PRINT *,'files that contains X_smooth,
Z_smooth, A_smooth, in'

C     PRINT *,'that order. The rows MUST be
organized so that the'

C     PRINT *,'profile is built from the mouth
to the head, with the'

C     PRINT *,'smallest value for X, and
largest value for A.'

C     PRINT *,'residing in the first row.
X_smooth and Z_smooth need'

C     PRINT *,'to be in m; A_smooth needs
to be in km2.'

C     PRINT *,' '

C     PRINT *,'Name of the first long profile
==>'

C     PRINT *, ' '

C     READ (*,'(A)') INFILE1

C     PRINT *,'Name of the second long
profile ==>'

C     PRINT *, ' '

C     READ (*,'(A)') INFILE2

C     PRINT *,'Name of the third long profile
==>'

C     PRINT *, ' '

C     READ (*,'(A)') INFILE3

C     PRINT *, ' '

C

      OPEN (UNIT=10, FILE='Owens4.csv')

      READ (10,*) XSTR, ZSTR, ASTR

      C=1

      XX(C)=XSTR

250   READ (10,*,END=260) X, Z, A

      C=C+1

         X1(C)=X

      X1INC(C)=ABS(XSTR-X)

      A1(C)=A*1000*1000

      XSTR=X

      GOTO 250

260   CONTINUE

C

      OPEN (UNIT=11, FILE='Owens2.csv')

      READ (11,*) XSTR, ZSTR, ASTR

      C=1

      XX(C)=XSTR

251   READ (11,*,END=261) X, Z, A

      C=C+1

         X2(C)=X

      X2INC(C)=ABS(XSTR-X)

      A2(C)=A*1000*1000

      XSTR=X

      GOTO 251

261   CONTINUE

C

      OPEN (UNIT=12, FILE='Owens3.csv')

      READ (12,*) XSTR, ZSTR, ASTR

      C=1

      XX(C)=XSTR

252   READ (12,*,END=262) X, Z, A

      C=C+1
```

```fortran
      X3(C)=X

      X3INC(C)=ABS(XSTR-X)

      A3(C)=A*1000*1000

      XSTR=X

      GOTO 252
 262  CONTINUE
C

      PRINT *, ' '
C

      LOW = 100000000

      J=-1

      DO 100, M=MSTART,MEND,MINC

      PRINT *, m

      J=J+2

      KDYN = KSTART

      DO 200 LCLOOP = 1,LOGCYCLE,1

      KK = KDYN*((10**LCLOOP)/10)

      KKK = KDYN*((10**LCLOOP)/10)*10

      H=0

      DO 300 K = KK, KKK, KK*KINC

      H=H+1
C

C

C    NOTE, in this case, all of the input files
will generate a C=100

C    therefore, in this next loop, we can go
from 2 to C.  But...if

C    the input rivers have a different
number of points in their
```

```fortran
C    profile, the code will have to be
modified to correctly generate

C    a counter that will execute the DO 400
loop correctly.

C

C

      DO 400 I=2,C,1

      IF (X1(I).LT.KP1) THEN

      DT=X1INC(I)/(K*(A1(I)**M))

      DT1=DT1+DT

      ENDIF

      IF (X2(I).LT.KP2) THEN

      DT=X2INC(I)/(K*(A2(I)**M))

      DT2=DT2+DT

      ENDIF

      IF (X3(I).LT.KP3) THEN

      DT=X3INC(I)/(K*(A3(I)**M))

      DT3=DT3+DT

      ENDIF
 400     CONTINUE


C

c     print *, dt1, dt2, dt3, m, k

C

      DT1=DT1-KPAGE1

      DT2=DT2-KPAGE1

      DT3=DT3-KPAGE1

C

c        misfit = (DIST**2)**0.5
```

```fortran
c        MISFIT=(DT1**2)**0.5

c        MISFIT=(DT1**2+DT2**2)**0.5

MISFIT=(DT1**2+DT2**2+DT3**2)**0.5

c        MPRINT (H,J) = K

c        MPRINT (H,J+1) = MISFIT

c        write (20,*) M, K, MISFIT

         IF (MISFIT.LT.LOW) THEN

          LOW = MISFIT

          KFIT = K

          MFIT = M

          MISLOG = LOG(MISFIT)

          print *, kfit, mfit, misfit, mislog

         ELSE

         ENDIF

        mislog = log(misfit)

c        print *, m, k, lcloop, misfit, mislog

        write (20, *) m, k, lcloop, misfit, mislog

         DT1=0

         DT2=0

         DT3=0

 300     CONTINUE

 200    CONTINUE

 100  CONTINUE

C

c     DO 500 P = 1, H, 1

c        WRITE (20,*) (MPRINT (P,Q),
MPRINT(P,Q+1), Q=1,J,2)

c 500  CONTINUE

        CLOSE (UNIT=20)

        CLOSE (UNIT=10)

        CLOSE (UNIT=11)

        CLOSE (UNIT=12)

        STOP

        END
```

**HELEN FITZGERALD MALENDA**
**927 Center Street | Floor 1**
**Bethlehem, PA 18018**
**(610) 246-3061 | hfm213@lehigh.edu**

EDUCATION

2014        Masters student, Lehigh University, *Bethlehem, Pennsylvania*

2011        B.S. Geology, Cumulative GPA: 4.0 Summa cum Laude, Kutztown University, *PA*


HONORS AND AWARDS

2015     Lehigh University Graduate Leadership Award

2014     National Science Foundation Graduate Research Fellow (NSF GRFP)

2013     Presidential Fellowship, *Lehigh University*

2011     Gold Medalist, Chambliss Award for Excellence in Research and Academics, *Kutztown University*

2005     Valedictorian, Class of 2005, *Fleetwood Area High School, Fleetwood, Pennsylvania*

RESEARCH INTERESTS

Geomorphology; river incision processes and landscape evolution; Quaternary geochronology and luminescence dating.

SELECTED PUBLICATIONS

**Malenda, H. F**., Raup, C.J., Pazzaglia, F.J., Berti, C., Harrison, R., Spears, D., 2014.  Surficial map and geomorphic study of South Anna River Deposits, Virginia: Investigating the presence of ongoing and cumulative deformation in the Central Virginia Seismic Zone, Scale 1:24,000. USGS EDMAP Award: G13AC0015.

**Malenda H.F.,** Pazzaglia, F.J., Berti, C., Nelson, M., Rittenour, T., Harrison, R. W., 2014. Investigating the presence of historical seismicity's effect on landscape evolution in the Central Virginia Seismic Zone, using fluvial stratigraphy and (paleo)geodesy [abs]: Geological Society of America-Annual Meeting inVancouver, British Columbia, Canada (19-23 October 2014) 272-14.

Simpson, E. L., Hennes, E., Bumby, A., Eriksson, P.G. Eriksson, K. A., Hilbert-Wolf, H. L., Linnevelt, S., **Malenda H. F.,**  Mondungwa, T., & Okafor, O. J., 2013, *Evidence for a 2.0 Ga continental microbial mat in a paleodesert setting.* Precambrian Research, v. 237, p. 36-50.


FIELD AND WORK EXPERIENCE

2013-2014     Surficial Geologic Map of the South Anna River in Ferncliff and Pendleton Quadrangles

2014             Tectonic Geomorphology Field Course, Northern Apennines, Italy, offered by ETH, CH

2014             Utah State University Luminescence Lab (one week)

Summer 2013   Teaching Assistant, EES 341, Geology Field Camp, Lehigh University

2012-2013     Staff Scientist, EarthRes Group, Inc. Pipersville, PA

2010             Grand Staircase-Escalante National Monument (GSENM), Utah (three weeks)

2010              Northern South Africa, Mpumalanga and Northwestern Regions (three weeks)


GRANTSMANSHIP

2014     NSF Doctoral Fellowship (NSF GRFP) $44,000/year for three years

2014     Geological Society of America Graduate Research Grant- $900

2014     Lehigh University Graduate Instruction Committee Research Grant- $2,000

PROFESSIONAL AFFILIATIONS

2014-  Full Member, Sigma Xi, The Scientific Research Society

2009-  Geological Society of America (GSA)

2013-  Women in Science and Engineering, (WISE) Lehigh University (treasurer: 2014-2015)